MART ANTON

Mechanical modeling of IPMC actuators at large deformations

Faculty of Mathematics and Computer Science, University of Tartu, Estonia

Dissertation is accepted for the commencement of the degree of Doctor of Philosophy (PhD) on May 08.05.2008 by the Council of the Institute of Computer Science, Faculty of Mathematics and Computer Science, University of Tartu.

Supervisors: Prof. Maarja Kruusmaa,
                   Tallinn University of Technology, Estonia

                   Prof. Alvo Aabloo, University of Tartu, Estonia

                   Jan Villemson, PhD, University of Tartu, Estonia

Opponents: Prof. Darwin Caldwell,
                   Italian Institute of Technology, Genova, Italy

                   Prof. Andrus Salupere,
                   Tallinn University of Technology, Estonia

Commencement: June 25, 2008 at the University of Tartu, Estonia

CONTENTS

LIST OF PUBLICATIONS

This Thesis is a summary based on the following papers, which are referred to in this text by their Roman numerals:

I   **A mechanical model of a non-uniform Ionomeric Polymer Metal Composite (IPMC) actuator.** M. Anton, A. Aabloo, A. Punning, M. Kruusmaa, Smart materials and structures, 17(2), pp 1–10, 2008.

II **Validating Usability of Ionomeric Polymer-Metal Composite Actuators for Real Life Applications.** M. Anton, A. Punning, A. Aabloo, M. Kruusmaa, (2006). IROS 2006, IEEE/RSJ International Conference on Intelligent Robots and Systems; Beijing, China; 9–15 October, 2006. IEEE, 2006. 1–6.

III **A Linked Manipulator with Ion-Polymer Metal Composite (IPMC) Joints for Soft- and Micromanipulation.** (2008) M. Kruusmaa, A. Hunt, A. Punning, M. Anton, A. Aabloo, ICRA 2008, IEEE International Conference on Robotics and Automation, Pasadena, California, 19–23 May, 2008. IEEE, 2008. 1–6.

IV **Towards a biomimetic EAP robot.** Towards Autonomous Robotic Systems (TAROS 2004); M. Anton, A. Punning, A. Aabloo, M. Listak, M. Kruusmaa, Clochester, UK; 06.–08.09.2004. Clochester, UK: University of Essex, 2004, (Technical Report Series), 1–7.

Patents pending:

V   **Linked manipulator**, Estonian Patent application, 08.03.2006, Tartu University; P200600005, Authors: Maarja Kruusmaa, Mart Anton, Andres Punning, Alvo Aabloo.

Other publications, relevant to my work but not included in this Thesis:

VI **Empirical model of a bending IPMC actuator.** A. Punning, M. Anton, M. Kruusmaa, A. Aabloo, Smart Structures and Materials 2006: Electroactive Polymer Actuators and Devices (EAPAD); San Diego, California, USA; 27.02.–02.03.2006. Bellingham: SPIE, 2006, (Proceedings of SPIE – The International Society for Optical Engineering), 61681V. 1–8.

VII   **A Distributed Model of IPMC.** A. Punning, U. Johanson, M. Anton, M.Kruusmaa, A.Aabloo, Smart Structures and Materials 2008: Electroactive Polymer Actuators and Devices (EAPAD); San Diego, California, USA; 10.03.–13.03.2008. Bellingham: SPIE, 2008, (Proceedings of SPIE – The International Society for Optical Engineering). 1–10.

VIII **A Biologically Inspired Ray-like Underwater Robot with Electro-active Polymer Pectoral Fins.** A. Punning, M. Anton, M. Kruusmaa, A. Aabloo, IEEE Confrence "Mechatronics and Robotics 2004" (MechRob04); Aachen, Germany; 13.–15.09.2004. Aachen: Eysoldt, 2004, (2), 241–245.

In publications [I,II,IV] the author has made the main contribution. The author has been responsible for modeling, experimental setup, experiments, analysis and writing the paper. The contribution of the author in [IV] is the conceptual design of the prototype and interpretation of the test results. The contribution of the author in [III] is the design of the linked manipulator as well as the analysis of the results.

ABSTRACT

An ionomeric polymer-metal composite (IPMC) material is a thin swollen polymer sheet covered with a metal layer from both sides. The sheet bends when voltage is applied to the metal surfaces.

This thesis investigates an IPMC actuator that consists of an IPMC sheet with a rigid elongation. It presents a novel nonlinear static mechanical model of an IPMC actuator. A situation where an IPMC sheet in a cantilever beam configuration pushes an object is modeled. The position of an object can vary along a circular trajectory. The IPMC sheet may also have a rigid extension attached to the top. The mechanical model of an IPMC actuator and its experimental verification are presented in Chapter 4 of this thesis.

Many electromechanical models have been presented in the literature. Their output parameter is an electrically induced bending moment (EIBM) or the load-free curvature of the sheet. Our mechanical model can take the output of those models as an input and calculate the position-force relationship of the actuator. The position-force characteristic permits an accurate engineering of various IPMC devices. Many authors have measured this characteristic, but only in the linear region. We measured and simulated the position-force relationship on a larger scale, where the relationship is nonlinear. As in other papers, the force is measured and modeled in a static equilibrium state. Measurement and modeling of dynamic output force remains a topic of a future study.

The model takes into account that the IPMC actuator may have an initial curvature and EIBM may vary along the sheet. The continuously changing curvature of the IPMC actuator can be computed using the model and algorithms presented in this thesis. When the IPMC actuator is pushing an object, the shape of the IPMC actuator tells us the direction of the force applied to the object. By comparing the shapes of the sheets at extreme opposite electric stimulations, one can learn how much the shape of the sheet can vary. It is harder to control the IPMC actuator which varies more. The properties of IPMC actuators with and without an elongation are discussed in section 4.2.

This thesis shows theoretically and experimentally that a rigid elongation increases linearity and controllability of an IPMC actuator. A summary of the advantages and disadvantages of elongated actuators are presented in conclusions in Section 6.1.

Finally, this thesis presents a design of a linked IPMC manipulator which is based on the findings of the theoretical and experimental work on IPMC modeling. It is shown that the design reduces the complexity of control and increases the precision and reaction speed of the device. The design of the linked manipulator and experiments are discussed in Chapter 5.

3

I   INTRODUCTION

This thesis presents a mechanical model of an IPMC (ionomeric polymer metal composite) actuator in a cantilever beam configuration. In the literature, IPMC (Ionic Polymer-Metal Composite or Ionomeric Polymer-Metal Composite) is also called ICPF (Ionic Conducting Polymer Film or Ionic Conducting Polymer gel Film).

IPMC is a type of an electroactive material that bends in electric field [1,2]. It consists of a thin (~200 µm) swollen polymer film with high ionic conductivity. One of the widely used materials is Nafion[TM], filled with water or ionic liquid. Both sides of the polymer film are plated with thin (~1µm) metal electrodes. Voltage applied between the surface electrodes causes migration of ions inside the structure of the polymer. The ion migration causes the volume change of surface layers of the polymer film. As a result of that effect the sheet bends (see Figure 1). The direction of bending depends on the polarity of the applied electric field.

(a)   (b)   (c)
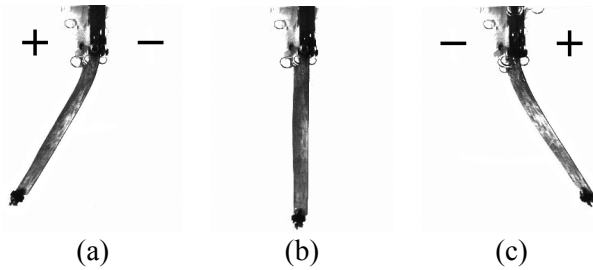
Figure 1. IPMC with (a and c) and without (b) electrical stimulation.

Electroactive behavior of an IPMC was discovered by Oguru, *et al*. [3] in 1992. From that onward researchers have been working on modeling IPMC actuators. The modeling of the IPMC actuator is a multi-physics task. It involves physical, chemical, electrical, electromechanical as also mechanical properties. Many electromechanical models have been proposed in the literature [VII,4,5,6,7,8,9,10]. They suggest that due to the applied voltage an electrically induced bending moment or change in free deflection curvature (in [10] it is called eigen-curvature) occurs. The mechanical model presented in this thesis can take electrically induced bending moment as an input. Output parameters of our model are the force and shape of the sheet.

The IPMC material has also sensing properties [11,12,13]. It is possible that an IPMC sheet is at the same time both a sensor and an actuator [14].

An IPMC actuator is characterized by large displacement. It is able to bend to form a circle or even beyond it. However, majority of models do not consider such large deformations. Our model gives the most detailed description of the

quasi-static mechanical behaviour of the actuator with a non-uniform bending at large deflections. We have also investigated a case where a part of the IPMC sheet is replaced with a rigid elongation. We will discuss the advantages of that particular design in the current thesis.

This thesis is organized as follows. Chapter 1 gives an overview of IPMC materials, state-of-the-art of their mechanical modeling and our research goals.

Chapter 2 describes the search for construction of the IPMC actuator which could be used to characterize the properties of the IPMC actuator and to validate the mechanical model that will be presented in Chapter 4.

Chapter 3 describes the role of the mechanical model in modeling the IPMC actuator.

Chapter 4 describes the mechanical model.

Chapter 5 describes an implication of the theoretical work described in this thesis. In particular, we describe a linked manipulator with IPMC joints.

1.1   Applications of IPMCs

The success of IPMC technology depends on whether or not suitable applications can be found. IPMC actuators have many good properties which makes them to an interesting option for novel actuator design. IPMC characteristics that could be considered advantageous, are:

1) Low driving voltages (less than 7V depending on the liquid used).
2) Large deflections (we have witnessed 5mm bending radius and less).
3) Fast response (the maximum load-free deflection in less than a second).
4) Softness (the equivalent elasticity modulus around 200MPa).
5) Small size (thickness around 0.2mm).
6) Durability (best IPMC sheets can last about a million bending cycles).
7) Low concentration of poisonous materials. The base polymer (Nafion/Flemion) and electrodes (precious metals like platinum, gold, etc.) are very stable and do not react with the surrounding environment.
8) The IPMC actuator is mechanically very simple and thereby IPMC actuators are relatively reliable and insensitive to damage.
9) IPMC technology is operational in harsh environments with low temperatures and vacuum conditions [15] provided that they are covered with a protective layer.

IPMC materials are relatively new and there are still many challenges regarding the applications of IPMCs. IPMC characteristics commonly considered disadvantageous are the following:

1) Small force/electrically induced bending moment (a piece of an IPMC with dimension 1cm×1cm can lift up one gram),
2) The risk of contamination. If the liquid inside the polymer gets contaminated, the performance of iIPMCs decreases.

Researchers are still seeking for an application niche for IPMC actuators. Mostly only laboratory demonstrations of concepts are discussed so far. According to our knowledge there exists only one commercial product – toy fishes – announced by EAMEX, Japan, at the SPIE's EAPAD 2003 Conference (see Figure 2). The video of the fish swimming can be downloaded from [16]. In [17] an overview can be found on how the materials are approaching commercialization.

Figure 2. A commercial product from Eamex Corporation, Japan. The tail of the fish is moved by IPMC.

Wide variety of applications has been proposed for IPMC actuators [18,19]. Please refer to [20] for a study of applicability of IPMC in space applications. IPMC actuators are considered as bio-compatible. For example, an active catheter system is proposed by Guo *et al* [21]. Yoon *et al* [22] propose IPMC as an actuator for a low-cost scanning fiber endoscope. Please refer to [23] for an overview of medical applications. The following two subsections describe the application of IPMC actuators for under-water vehicles and for soft- and micromanipulation.

1.1.1   Under-water vehicles

IPMC actuators can be suited for underwater technology because of a low driving voltage (reduced risk of short-circuit through water) and large deflection (effective underwater propulsion). The risk of contamination and drying is usually avoided by restricting the working conditions to de-ionized water. The sheet could also be coated with additional polymeric layers [24] to protect a material from contamination.

In addition to the commercial product mentioned above, many proof of concept designs have been proposed. In this short review only few are mentioned. Anton *et al* [IV] propose a ray-form swimming robot which uses pectoral fins to propel itself forward. This ray has 2 pairs of IPMC actuators. The design is described in more detail in section 2.1. Punning *et al* [VIII]

present a similar robotic ray which utilizes 8 pairs of IPMC actuators (see Figure 3). Due to the use of IPMC actuators, the design is much simpler than for a ray that utilizes DC motors [25]. A snake-like swimming robot is introduced by Ogawa *et al* [26]. An autonomous controllable fish is demonstrated by Mbemmo *et al* [27]. An undulatory tadpole robot is demonstrated by Kim *et al* [28].
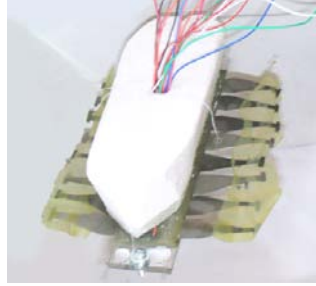
Figure 3. The device which utilizes 8 pairs of IPMC actuators.

1.1.2 Soft and micro micromanipulation

Because of large deflections, softness and small thickness IPMC actuators are considered as a strong candidate for soft- and micromanipulation. Lumia and Shahinpoor [29] describe a design of a micro-gripper. Chen *et al* [30] propose an application of IPMCs for micro-injection of living Drosophila embryos. Nakabo *et al* [31] describe a two-dimensional (2-D) multi-degree-of-freedom (DOF) robot manipulator made from IPMC (see Figure 4).

Figure 4. Application of a multi-DOF micro-manipulator with an IPMC artificial muscle and with visual feedback control proposed by Nakabo *et al* [31].

Tadokoro *et al*. [32] have proposed an elliptic friction drive element consisting of an arch-shaped IPMC. As a follow-up to that work, Tadokoro *et al*. [33] fabricated a multi-DOF micromanipulator. It consists of two friction drive elements.

1.2 The mechanical models of IPMC actuators

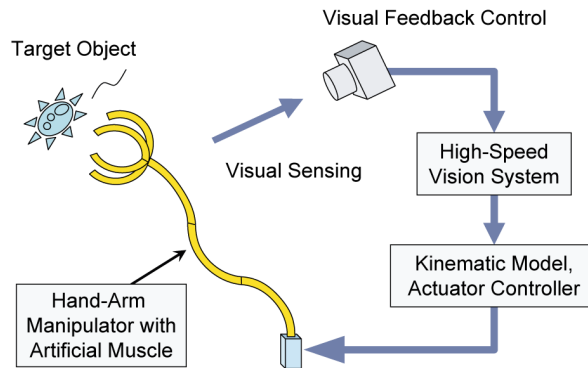Various mechanical models of IPMCs or other bending EAP-s have been developed by a number of authors, emphasizing different features [5,6,34,35,36,37,38,39,40,41,42]. Table 1 summarizes features relevant to modeling of IPMCs. Table 2 represents the comparison of previously described models of the IPMC and our work [I] on the basis of whether they address the features in Table 1. Besides the features depicted in the table, the models can also differ by other details. In Table 3 main features are listed for each of the papers.

Table 1. Features relevant to the modeling of IPMCs

	Feature	Description
1	Non uniform bending	Only free bending curvature can be considered to be approximately constant but even then only if EIBM is constant and the IPMC sheet moves slowly. As soon as the IPMC sheet is loaded, the curvature will vary along the sheet.
2	Initial Curvature	IPMC sheets may be initially curved even when neither force nor electric current is applied (see Table 4). Alternatively, the model may be suited to describe only nearly perfectly straight IPMC sheets.
3	Large deformations	Models that do not support large deformations have a gradually increasing modeling error as the deflection angle increases (see Figure 5). In case of 90 degrees deflection angle the modeling error becomes clearly notable. Therefore, deformations that result in deflection angles larger than 90 degrees can be considered large.
4	Non uniform EIBM	Several authors report that EIBM varies along the sheet [VI,43,44]. Alternatively, in case of small pieces of an IPMC, small currents and good electrode layers the EIBM can be considered uniform.
5	Force output	IPMC actuators can be used to apply force to an object (e.g. load cell). Alternatively, only a free bending of the IPMC sheet may be modeled.
6	Varying load position	An IPMC actuator works while pushing an object along a trajectory. So the IPMC sheet applies force to the object in different positions. Alternatively, force may be determined only on the same plane with the contacts.

7	Elongation	A rigid elongation may be attached to the top of the IPMC sheet. Advantages of an elongation have been discussed by Campolo *et al* [45]. Some new advantages are presented in this thesis. For example, we will show that an elongation can be used to increase linearity and controllability of IPMC actuators.
8	Linearity	Linear models can be defined by linear differential equations. Linearity is a very useful feature if one wants to control the IPMC sheet in real time.
9	Dynamic behavior	The model should describe the movements of IPMC sheet. Alternatively, the model may only describe the static equilibrium of the IPMC sheet. This kind of a model can be used to describe quasi-static movements of the sheet – movements that are so slow that inertial and drag forces can be neglected.

Table 2. Comparison of our model with those from the literature on the basis of whether they address the features in Table 1

	Feature	[I]	[5]	[6]	[34]	[35]	[36]	[37]	[38]	[39]	[40]	[41]	[42]
1	Non uniform bending	✓	✓	✓	✓	✓	✓		✓		✓	✓	✓
2	Initial Curvature	✓								✓			
3	Large deformations	✓			✓				✓	✓			
4	Non uniform EIBM	✓							✓			✓	
5	Force output	✓	✓	✓	✓	✓	✓	✓					
6	Varying Load position	✓			✓	✓							
7	Elongation	✓							✓				
8	Linearity		✓	✓			✓	✓				✓	
9	Dynamic behavior			✓			✓		✓		✓	✓	

Table 3. Additional features of the models in the literature

Paper	Main features described in the paper
Tamagawa *et al* [5]	Reports time-dependant nominal Young modulus which is proportional to bending stiffness, and presents a method to estimate it.
Yagasaki and Tamagawa [6]	The work improves the work by Tamagawa *et al* [5] by additionally considering viscoelastic properties of IPMC sheets and the time-dependent properties of EIBM.
Bao *et al* [34]	Demonstrates that under applied voltage an electric-field unimorph EAP (made of stretched electron irradiated P(VDF-TrFE) copolymer) can develop a deflection angle of 360 degrees. The work also presents a model to describe such large deformations.
Sangki *et al* [35]	Proposes an equivalent bimorph beam model and an equivalent beam model. In case of an equivalent bimorph beam model the IPMC is assumed to have two virtual layers. Under applied voltage the upper layer and the lower layer of an IPMC expand or contract respectively to produce the IPMC's bending motion. For the numerical analysis, a commercial finite element analysis program – MSC/NASTRAN – was used.
Huynh *et al* [37]	Proposes a mechanical design of a robotic finger and then assembles two of the fingers to form a robotic gripping system. The system is experimentally evaluated The material studied is polypyrrole (PPy).
Yim *et al* [38]	The IPMC sheet is divided into constant curvature segments. Each of the segments is controlled individually. State space equations are found which couple the applied voltage to curvature for each fo the segments. It is not possible to find a linear relationship between voltages and tip deflection with this approach.
González and Llorca [39]	As all the other studies focus on normal loads, this paper considers axial loads to curved beams. The material studied is polyethylene felt. It is a non-electroactive material, but the theory still applies to electroactive materials also.
Pugal *et al* [40]	Considers self-oscillating IPMCs. Self-oscillation is caused by electrochemical reactions on the platinum electrode of an IPMC sheet. The modeling technique is Finite Element method (FEM).
Chen and Tan [41]	A two block model structure for an IPMC actuator is proposed consisting of electromechanical and mechanical blocks. A linear static beam theory [46] is used in conjunction with a dedicated white box electromechanical model. The model enables controler design while capturing fundamental physics. An H-infinity controller is built and successfully tested.

Newbury [36]	The paper presents a complete model of an IPMC incorporating electrical, electromechanical and electrical terms. Also force-displacement relationship is studied. In case of small deformations, the force-displacement relationship was observed to be linear.
Samaranayake *et al* [42]	Classical linear beam theory is used to model the behavior of the IPMC sheet but its precision is improved by also taking into account the horizontal displacement.

As it can be seen from Table 2, linear models do not support large deformations. This is because linear models make use of classical linear beam theory [46] but classical linear beam theory neglects the axial displacement of the beam. In Figure 5 one can see a comparison of beam shapes under different normal loads according to linear and nonlinear beam theory. One can see that the length of the beam, according to the linear theory, becomes longer as the deformation increases. For details of the simulation please refer to appendix A.
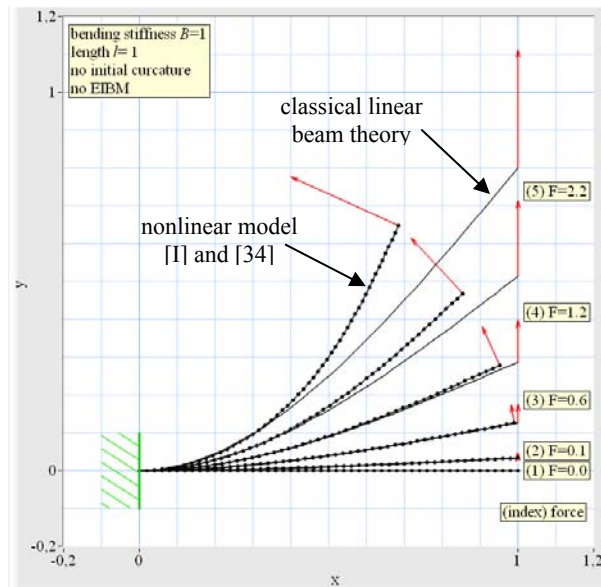

Figure 5. Beam deformations under different concentrated normal loads according to linear and nonlinear beam theory.

1.3 Research goals and Contributions

As it can be seen from Table 2, to date no model has all the features listed in Table 1. Our model has most of the features. It only lacks linearity and dynamic behavior.

17

Linearity has its limitations. Linear beam theory is not able to describe large deformations as delineated in Figure 6. Linear beam theory could be, with some considerable modeling error, be applied in configurations (1-3), but is unable to accurately describe configurations (4–9). Please refer appendix A for details of the calculations.
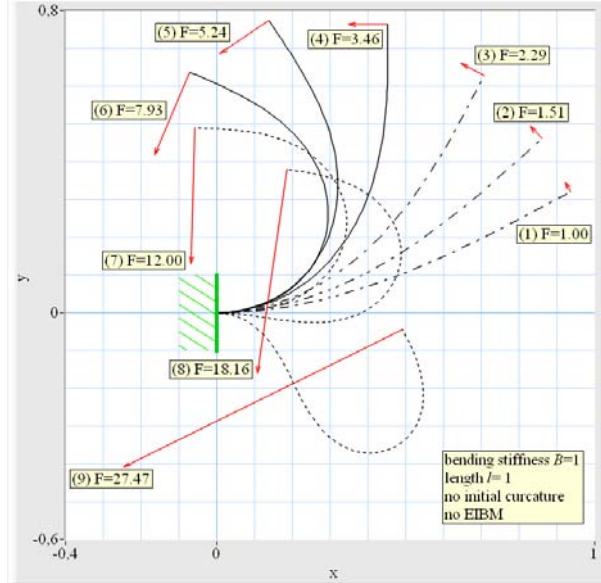

Figure 6. Deflections of the cantilever beam under different normal loads.

An IPMC actuator is a dynamic system. The shape and the output force are time-dependent. However, if all the parameters are held constant, the sheet would soon attain a static equilibrium state. In paper [I] and in this thesis we propose a mechanical model to describe the shape and the output force of the IPMC actuator in that state. The model can be used to describe quasi-static movements of an IPMC sheet – movements that are so slow that inertial and drag forces can be neglected.

The contribution of the thesis with respect to the previous work is the following:

- A simple ray shaped robotic fish is proposed. It utilizes 2 pairs of IPMC sheets. Using that prototype the feasibility of IPMC actuators is demonstrated. The design of the robotic fish and the experiments are discussed in section 2.1.
- A system for testing the usability of IPMC actuators for precision control tasks – an inverted pendulum system – is proposed. We also present a simple empirical model that is able to hold the pendulum up to 10s. To our

knowledge, this is the first attempt to control an inherently unstable system with IMPC actuators. This is the contents of section 2.2.

- A testbed for IPMC actuators is presented. It enables studing the behavior and characterizing the properties of IPMC actuators. It enables determining the bending stiffness and EIBM of an IPMC actuator. It also enables measuring the position-force relationship which is an important characteristic for mechanical design of IPMC devices. The system also enables studing the behavior of IPMC actuators consisting of an IPMC piece and a rigid elongation attached to it. The testbed is presented in section 2.3.

- A structure of the model of an IPMC actuator and an explanation of the role of the mechanical model on modeling IPMC actuators is proposed. A modular approach to IPMC actuator modeling is described in Chapter 3.

- A new mechanical model of an IPMC actuator is presented. It describes quasi-static movements of the IPMC actuator in cantilever configuration at large deformations. The model considers a possible asymmetry of the IPMC material. The IPMC actuator may have an initial curvature and EIBM may vary along the sheet. The model also permits usage of a rigid elongation attached to the top of the IPMC sheet. This gives designers more options for customizing the properties of the actuator. Using the model one can compute the force-deflection characteristic of any described IPMC actuator. The mechanical model and its experimental verification are presented in Chapter 4.

- An elongation as a tool for increasing controllability and linearity of IPMC actuators is introduced. The impact of elongation to IPMC actuator properties is discussed in sections 2.2.4, 4.2, 4.3 and summarized in section 6.1.

- A design of a linked manipulator and its characterization are described. It was observed that this design increases not only the reachable workspace, but also precision and reaction time of the actuator. The design of the linked manipulator and experiments are presented in Chapter 5.

1.4 Technical note

The IPMC used in the experiments is a commercial product of BioMimetics Inc. called MuscleSheet™ with Pt surface electrodes and Na^+ doping ions. MuscleSheet™ is about 0.2 mm thick. The thickness of Pt surface electrodes is approximately 0.01mm. Due to an imperfect fabrication procedure the material is asymmetrical. It has an initial curvature and different electrode thickness on different sides. The properties of the material vary from sample to sample.

2 THE CONSTRUCTION OF AN IPMC ACTUATOR AND ITS MEASUREMENT METHODOLOGY

This chapter describes our search for design of the IPMC actuator which could be used to characterize the properties of the IPMC actuator and to validate the mechanical model that will be presented in Chapter 4.

As described in section 1.1., an IPMC actuator can have many applications and different designs. One of the possible applications are fins for a robotic fish. The second application is an inverted pendulum system for investigating the controllability of and IPMC actuator. The third application is the manipulation of an object moving along a circular trajectory. These possible applications are studied in the following sections.

2.1 Robotic fish

This section describes a feasibility study of IPMC actuators based on a simple robotic fish prototype.

One of the possible applications of IPMC actuators are fins for a robotic fish. This is an example of utilization of IPMC's unique properties. A fin as pictured in Figure 7 is very simple as there is no overhead equipment (such as gears and lever mechanisms). If one applies electric voltage to the IPMC sheets, the fin bends. If one applies voltage with predetermined phase shifts between the IPMC sheets, the fin generates thrust.
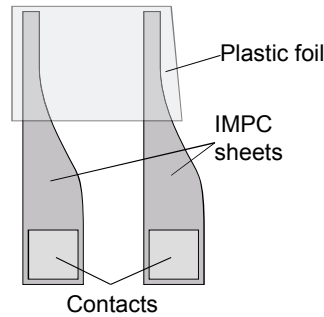

Figure 7. A pectoral fin utilizing IPMC actuators.

Many designs for a robotic fish have been proposed in the literature [28,26,27]. The research in [IV] reports preliminary attempts to build a biomimetic fish-like EAP robot. The aim of the research is twofold. First, we aim at using the robot as a testbed for the development of IPMC control

algorithms. The second aim is replication of the undulating motions of ray fins to discover effective ways of locomotion of biomimetic underwater vehicles.

2.1.1 System setup

The experimental setup is presented in Figure 8. The robot consists of two pectoral fins on both sides of a 0.5 mm thick plastic frame. The size of the frame is 27 mm × 35 mm. The frame is used to attach the gold contacts tightly against the platinum coating of the IPMC sheets. The body is made buoyant by fixing the frame under a piece of expanded polystyrene. The device lies in a tank filled with deionized water. The weight of the robot is 9,6g. The weight of the fins (wet IPMC sheets and the plastic foil) is 1,5g.
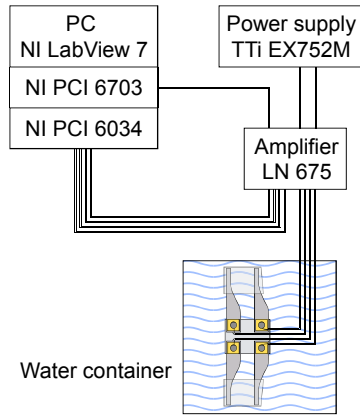

Figure 8. The experimental setup for the robotic fish.

The experiments were recorded with a digital video camera. A ruler was drawn to the background to enable measuring the speed of the fish.

2.1.2 The robot ray control algorithm

A program for controlling the motion of the fins was created by LabView 7.0. Please refer to [47] for the source code. A pectoral fin of the robotic ray as pictured in Figure 7 consists of two individually controllable IPMC sheets. The program computes and applies voltage to the two IPMC sheets in real time. It enables changing the frequency and phase shift of the IPMC sheets on the run. The same signal is applied to both pectoral fins and they move synchronously.

The algorithm applying voltage to the IPMC sheets is presented in the form of a dataflow diagram or Block Diagram (see Figure 9) as it is called in

LabView. It contains a loop which iterates until stop button is pressed. In each iteration the value of controls (like stop button) inside the control loop in the block diagram is checked. The value of controls (like waveform) outside the control loop is checked only at the beginning of the execution. The values of controls can be defined on Front Panel (see Figure 10). In each iteration indices are computed and corresponding voltages read from the waveform. The voltages are then applied to the IPMC sheets using a device interface provided by LabView.
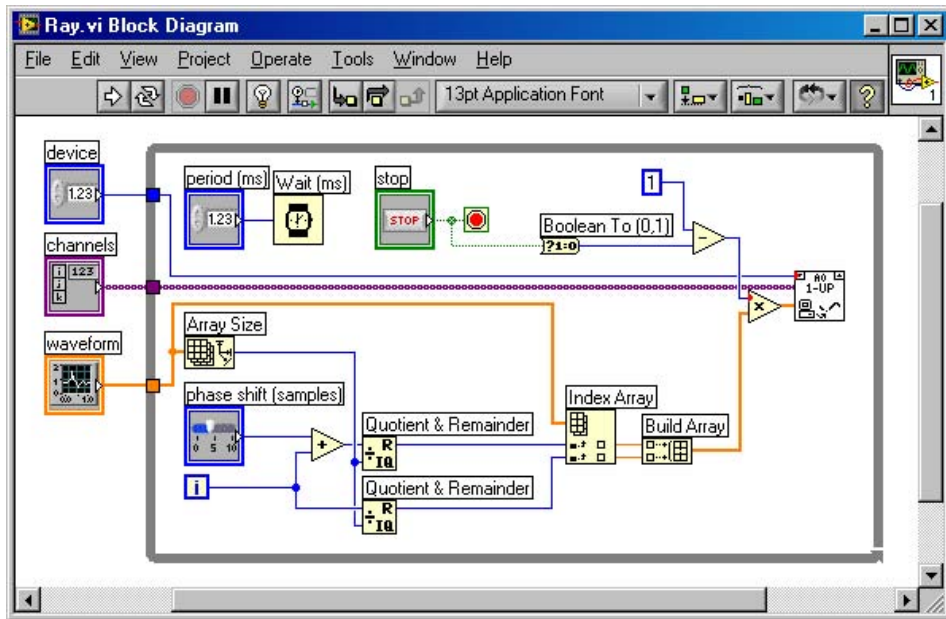

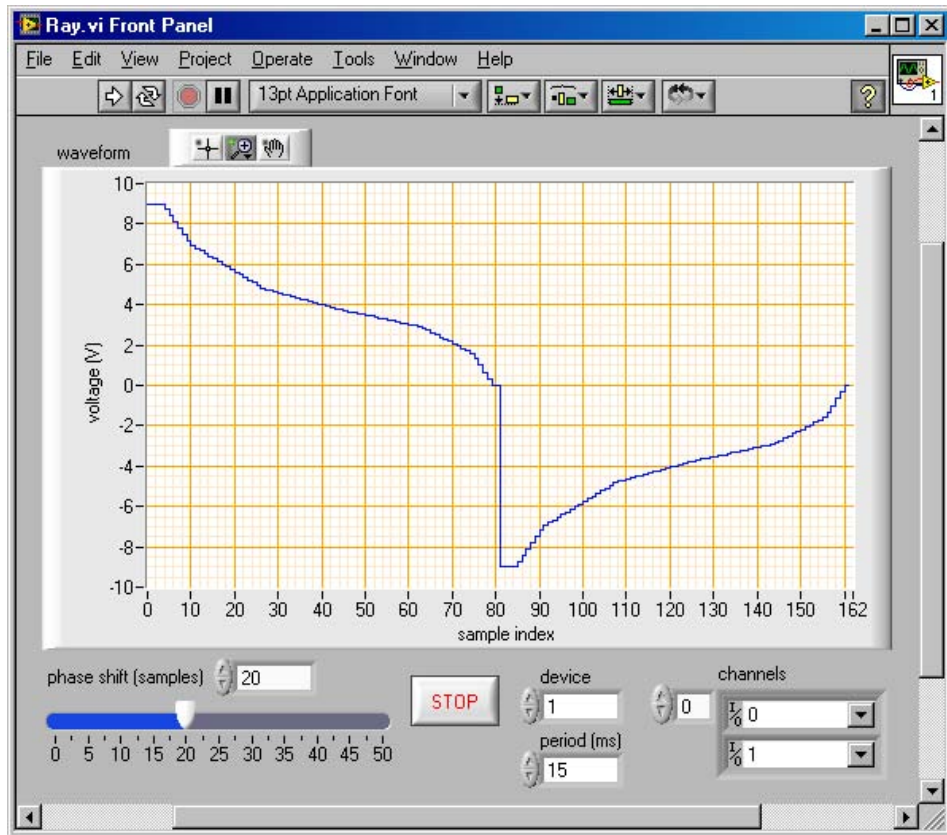**Figure 9.** The block diagram of the algorithm.

Figure 10. Front Panel with controls of the algorithm.

2.1.3 Experimental results and discussion

The main result of the experiments is that the fins are able to generate thrust and move the body forward. The speed of the robot varied in different experiments from approximately 3mm/s to 9 mm/s. Please refer to [48] for videos of experiments. It can be concluded that rajiform swimming can be effectively mimicked with the help of EAP muscles. In Figure 11 one can see a photo of that robot floating in the tank.
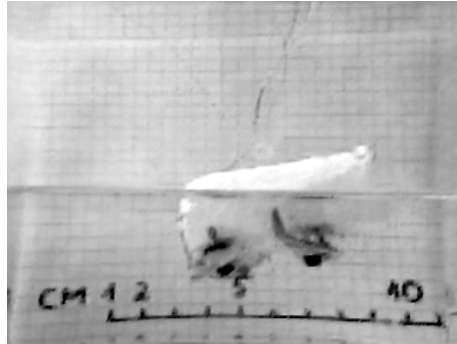
Figure 11. Photo of the robot floating in the tank. A self-made ruler can be seen on the background.

The mechanical design of the fins was found reliable but the largely varying properties of the EAP muscles made the robot unstable. Feedback control could help to move the fins as desired. However, the system setup did not permit measuring the movements of fins easily. In the next section an application of IPMC actuators is proposed, which makes the performance of IPMC actuators easier to measure.

2.2 An inverted pendulum system

In [II] a test application of IPMC actuators – an inverted pendulum system – is proposed, which is easier to monitor and characterize than a fin of a ray-like robotic fish. Many possible applications of IPMC actuators, such as robotic arms, require great precision from actuators. This test application proposed enables examining IMPC actuators from the point of view of precision control.
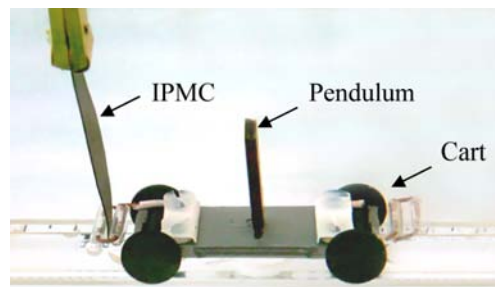

Figure 12. Inverted pendulum system.

The inverted pendulum system is presented in Figure 12. It consists of a moving platform, a pendulum and an IPMC actuator, which pulls and pushes

the platform. The goal is to maintain zero deflection angle of the pendulum and zero position of the platform. An inverted pendulum system is inherently unstable. The pendulum will not stay upright by itself. The IPMC actuator has to work constantly to keep the pendulum up. Assessing whether the system has been successfully controlled is therefore a trivial question. If the pendulum is held up and deviations form the initial position of the platform are kept small, the control can be considered successful.

2.2.1   System setup

The setup of the system is presented in Figure 13. A clamp, with golden jaws holds the sheet in cantilever configuration and enables applying voltage to it. To keep the IPMC strip hydrated, the system is placed in a tank of deionized water. The IPMC strip is controlled by a PC running National Instruments LabView 7.0. To assure frictionless contact between the IPMC actuator and the platform, the platform holds the actuator between two rolls. A monochrome camera JAI-235 is used to film the experiment with the frame rate 25fps. The image from the camera is used to determine the position of the platform and the angle of the pendulum. Please refer to [II] for more details about the system setup.
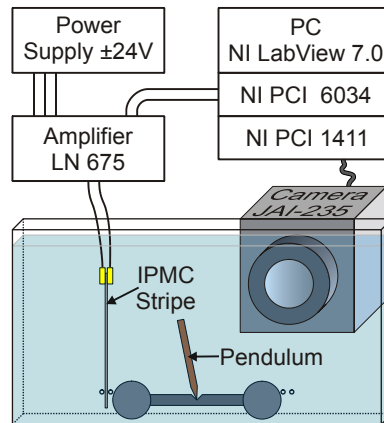

Figure 13. The setup of the inverted pendulum system.

2.2.2   An inverted pendulum control algorithm

A program was developed in LabView 7.0 for conducting experiments with the setup described in the previous section. Please refer to [49] for the source code. The program does the following:

1. Hardware control.
   1.1. Acquiring images from the camera using image acquisition card NI PCI 1411.
   1.2. Writing the computed voltage response to the Input-Output card NI PCI 6034.
2. Computing the voltage to be applied to the IPMC sheet.
   2.1. Analyzing the acquired image and computing:
      2.1.1. The position of the platform.
      2.1.2. The angle of the pendulum.
      2.1.3. Whether the pendulum has been released and moving freely.
   2.2. Estimating the velocity of the platform and the angle of the pendulum.
   2.3. Based on the state of the platform and pendulum, calculating the voltage to be applied to the IPMC sheet.
3. Saving the input and output data
   3.1. Storing the parameters of the system and the response of the controller to LabView measurement file (*.lvm).
   3.2. Creating an unpacked video file (*.avi) containing the video of the experiment.

The program computes and applies voltage to the IPMC sheet in real time at fixed intervals after every 0.04s. In the beginning of the execution it is possible to calibrate and test the image acquisition hardware and image analysis software. Afterwards the program is fully autonomous, however it can be stopped any time by pressing the stop button.

To determine the voltage to be applied to the IPMC sheet we need to know the state of the platform and the pendulum. The state of the platform and the pendulum is represented by four variables:

1. position of the platform,
2. angle (0 if vertical) of the pendulum,
3. velocity of the platform and
4. angular velocity of the pendulum.

Image analysis gives us only the position and the angle. The velocities have to be calculated. This is challenging mostly because of the low sampling rate of the positions.

The velocity of the platform is calculated using a position reading from the previous interaction. It means that the algorithm has to remember the previous state. The velocity is approximated with an average velocity between two positions.

It means that we assume zero acceleration. This assumption does actually not hold. The velocity can change considerably in 0.04s (duration of one iteration). However, as we do not know the actual acceleration, zero acceleration is our best bet. Acceleration can not be approximated using a longer

history of former readings of the position, because also the acceleration changes considerably in 0.04s.

Because we are unable to estimate the acceleration of the platform, we are not able to estimate the force applied to the platform either.

As an attempt to reduce chaotic fluctuations of the velocity, a simple low-pass filter was applied to the velocity signal. The computation of velocity of the platform and of the angular velocity of the pendulum is done in the same way.

The task of calculating the voltage to be applied to the IPMC sheet can be divided into two stages. In the first stage the force to be applied to the cart in order to balance the pendulum is found. Please see [II] for more details. In the second stage the electric voltage to be applied to the IMPC strip in order to achieve the desired force is found. Accordingly, the controller of the system consists of two parts (Figure 14).
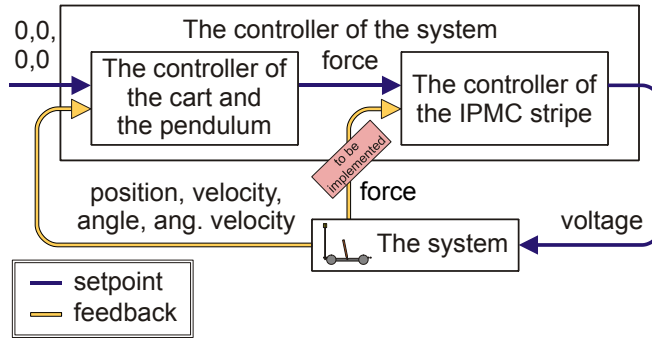

Figure 14. Block diagram of the controller

Many successful attempts to precisely control the output force of IPMC actuators are reported in the literature [7,41,50,51,52,53,54]. However, they all control an IPMC actuator in air, in a feedback manner and they control the free deflection or force in only one position. These constraints are not satisfied in our case. We used a very simple empirical model to control the output force of the IPMC actuator. Please see [II] for more details.

2.2.3   Contact free measuring of the state of the system

The position of the platform and the angle of the pendulum are determined from the image of the monochrome camera. The resolution of the image was 320x240 pixels. The position of the objects is found by analyzing corresponding pixel rows on the image (see Figure 15).
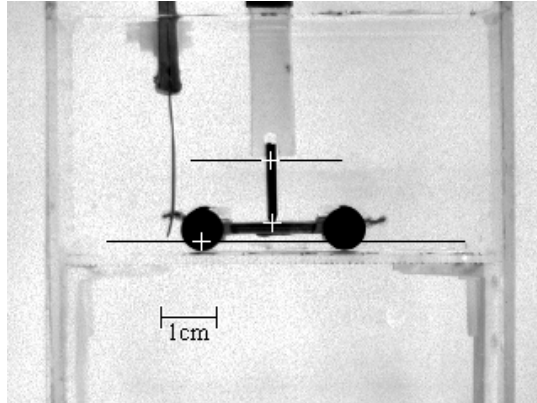
Figure 15. An image from the camera and the two pixel rows of interest. The positions of the left wheel and the pendulum, found by the image analysis software, are marked with white crosses. The location of the joint of the pendulum calculated based on the position of the left wheel is also marked with a white cross.

Luminosity graph corresponding to the upper row is presented in Figure 16. One can see the raw luminosity signal and the filtered signal. The pendulum and the wheel are black and differ clearly from the white background. The minimum point of the filtered signal corresponds to the position of the pendulum on that particular row. The calculation of the pendulum angle is a matter of simple trigonometry. To filter the raw luminosity signal a filter was used. It consisted of two moving averages subtracted from each other. Peak detection algorithm was provided by LabView.
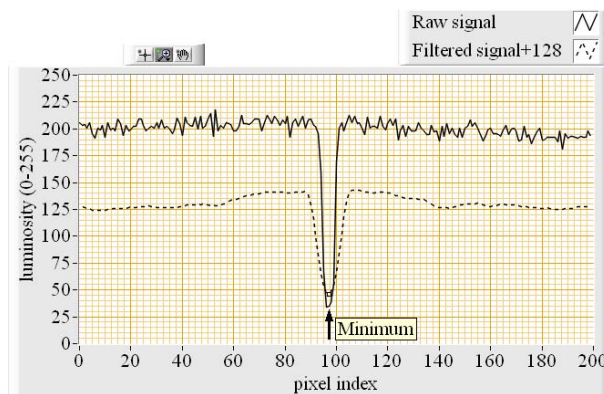

Figure 16. Luminosity graph of the upper pixel row in Figure 15.

The position of the platform is found similarly to the angle of the pendulum.

Also a fork which holds the pendulum can be seen on the image from the camera (see Figure 15). We want to start the experiment by pulling the fork up and releasing the pendulum. This can be detected by monitoring luminosity of a certain pixel on the topmost pixel row. A black rubber band is attached to the fork for that purpose. If the luminosity changes from black to gray, the fork has been removed.

2.2.4   Experimental results and discussion

A video [55] presents the preliminary experiments with IPMC control of the inverted pendulum system described above. Despite of the insufficient sampling rate of the camera, the pendulum could be balanced for up to 10 sec. We believe that the results of controlling the system can be improved by sampling the input data with higher frame rate. It would enable to obtain better estimates of velocity and force. For more details about the experiment please refer to [II]. A graph with the position of the platform and the angle of the pendulum is presented in Figure 17.
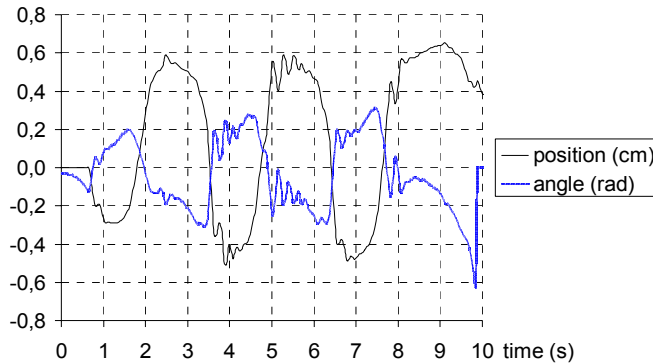

Figure 17. A waveform chart of the position of the platform and the pendulum angle during the experiment.

Three snapshots of the experiment are presented in Figure 18. One can see a peak forming in the middle of the sheet. This is due to curving in multiple directions as presented in Figure 19. As explained in [10], no direction is preferred when IPMC sheet curves. The direction of curving is determined by mechanical constraints like the clamp.
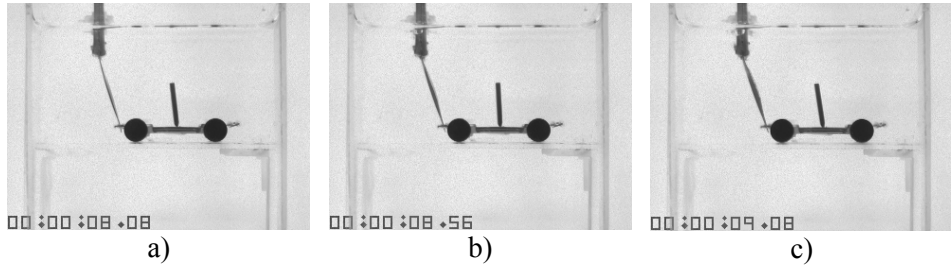
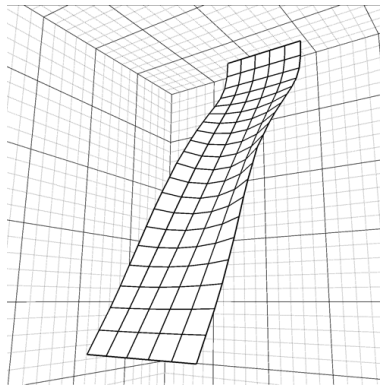**Figure 18.** Three frames from the video "experiment01.mpg".

Figure 19. Drawing of the shape of the sheet in Figure 18 (c).

We noticed that the sheet mainly curves near the contacts. This gave me the idea to replace the top part of the IPMC sheet with a plastic elongation (see Figure 20). Also, an elongation precludes curving in multiple directions.
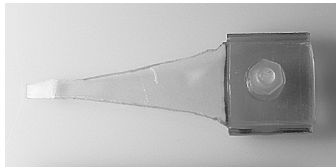

Figure 20. The elongation used to replace top part of the sheet.

Consecutive frames from experiments with an elongated sheet are presented in Figure 21. At the moment suitable parameters for controlling the elongated sheet where not identified because of the complexity of the process. This problem originates from the nature of empirical models.
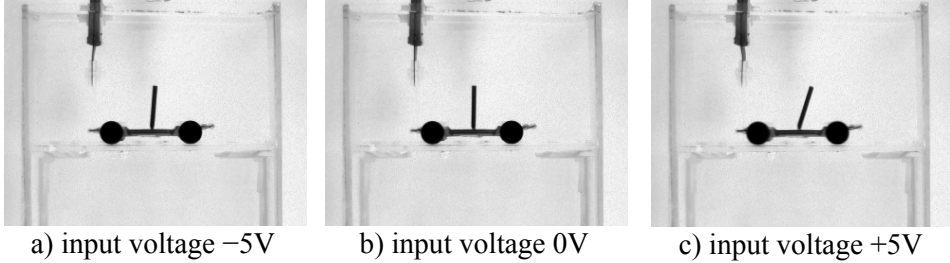
a) input voltage −5V   b) input voltage 0V   c) input voltage +5V

Figure 21. An elongated sheet controlling the position of the platform. Please note that the shape of the sheet depends on the driving voltage.

Empirical models are not geometrically scalable. If the length of the IPMC strip changes, one has to find new values for all the parameters. That means extensive experimentation, which in our case is very time-consuming. A solution would be the use of a physical model. One can notice in Figure 21 that in the same position the IPMC sheet can have different shapes. A physical model could explain that phenomenon.

As the first step in building the physical model we have identified that the IPMC actuator is a three port system. Not only does the output force depend on the applied voltage, but due to its stiffness it also depends on the position of the actuator. The corresponding schema of the actuator is presented in Figure 22.
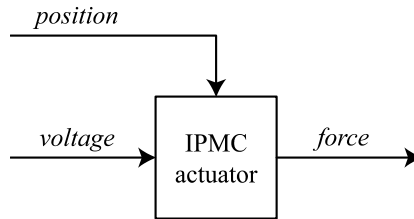
Figure 22. A schema of the IPMC actuator for predicting the output force.

2.3   A testbed for IPMC actuators

In this section a testbed for IPMC actuators is presented. An IPMC sheet between contacts and possibly with a rigid elongation applies force to the load cell. It is very similar to the inverted pendulum task, only the trajectory is now circular and the platform is replaced by a load cell to measure output force of the actuator. The aim is to measure the force along a circular trajectory to get the force-displacement relationship of the actuator. The force-displacement characterisitic is important when designing IPMC devices.

The force-displacement characteristic is also measured in [35,36]. However, in these papers an IPMC actuator was not in a permanent contact with the load cell. It could bend freely until it touched the load cell. This approach is not well suited for measuring the force in case of large deformations for the following reasons:

1. In case the distance to the load cell is long, an IPMC actuator would gain momentum and tip the very sensitive load cell. The sudden impulse of mechanical energy causes oscillation of the load cell readings.
2. An IPMC actuator exhibits back-relaxation [1]. In case the distance to the load cell is long, it will take time for the actuator to reach the load cell and the peak force is missed at the time of the measurement.
3. It may happen that the load cell is too far away and the IPMC actuator will not reach it. The solution would be to place the load cell on the other side of the IPMC actuator. Figuring out on which side to put the load cell would complicate the experiments.

A system setup that overcomes the problems listed above is presented in chapter 2.3.1. The methodology of the sheet shape measurement is discussed in chapter 2.3.2. The two different actuator configurations studied in this thesis are presented in Chapter 2.3.3.

2.3.1 System Setup

The system setup is presented in Figure 23. An IPMC actuator in cantilever configuration applies force to a load cell. The tests were conducted in air, so the IPMC strip had to be moistened between experiments. The voltage applied to the actuator was controlled with a PC running LabView 7. The measured force and image of the system are processed by the same computer. The image from the camera is used to determine the shape of the sheet. Please refer to section 2.3.2 for details about image analysis.
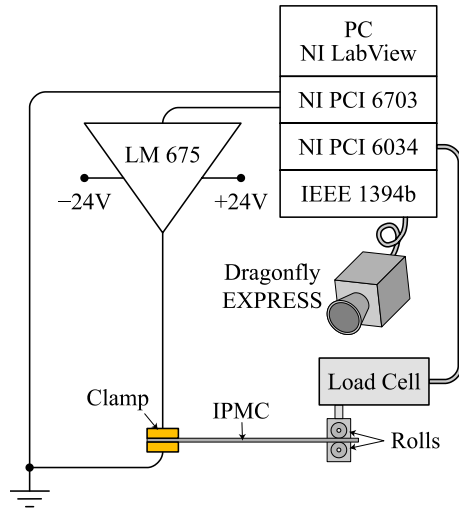
Figure 23. The setup of the testbed.

Force applied by the IPMC actuator was measured with the Transducer Techniques GSO-10 load cell. The load cell can be placed anywhere along a circular trajectory. In the experiments discussed in this paper the radius of the trajectory is 40mm and the force is measured in 7 positions as they are marked in Figure 24. The IPMC actuator bends horizontally, so gravitation will not affect its movement.

Figure 24. Positions on the trajectory where force and shape of the sheet are measured.

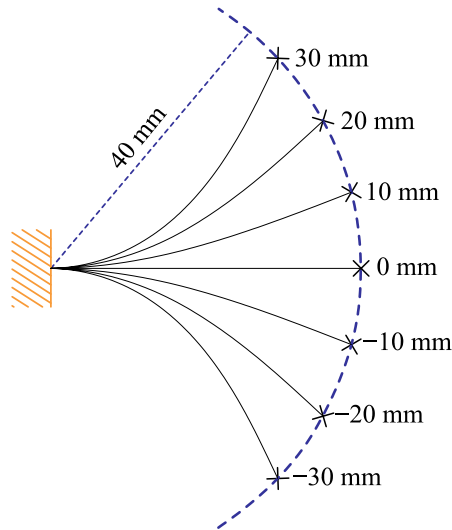Different from methodology in [35,36], the actuator was steadily connected to the load cell. This enabled measuring force even in those positions, which the IPMC strip would not reach if it was bending freely. To ensure a frictionless contact, the tip of the actuator was held between two rolls.

Please refer to [I] for more details about the system setup.

2.3.2 Contact-free measurement of the shape of the sheet

The shape of the sheet can be determined from the camera image (see Figure 25). The resolution of the image is 640x480 pixels. Ten images are saved synchronously with force measurements. The mean of the ten images is used for image analysis. This operation may cause motion blur as can be seen in Figure 25.
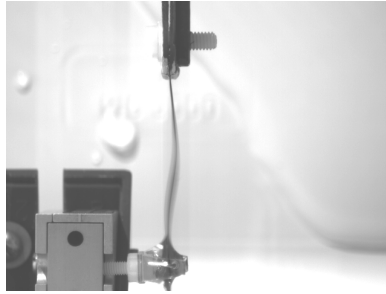
Figure 25. A videoframe from the camera. Note that the IPMC sheet is vague in the middle because of the motion blur.

Many methods for characterization of the shape of IPMC actuator have been proposed by various authors.

Punning *et al* [VI] proposed a very simple intuitive method for characterization of the shape of the IPMC sheet. The contour of the actuator on the image is divided into vectors with equal lengths as shown in Figure 26. For each vector angle a_i between the current and the previous vector is registered. The vector of changing angles $a_1,...,a_n$ describes the bending movement of the actuator. However, this method does not permit estimating the curvature very precisely.

Figure 26. The shape of the sheet is represented through a vector of angles.
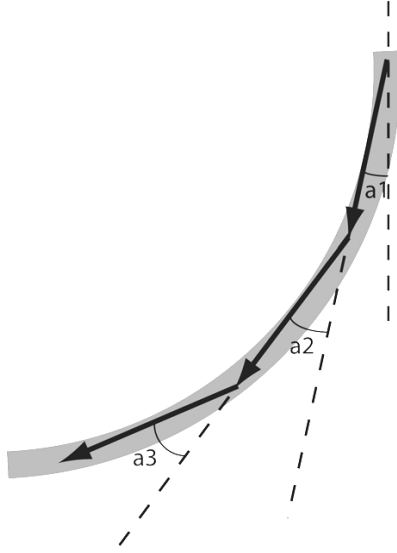
Bar-Cohen *et al* [56] proposed a method which assumes that the curvature of the IPMC sheet is constant. This assumption is not valid in our case.
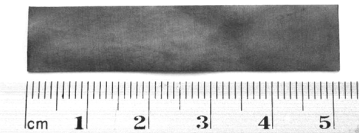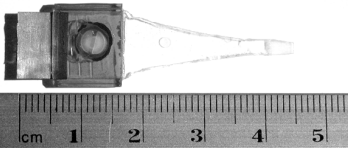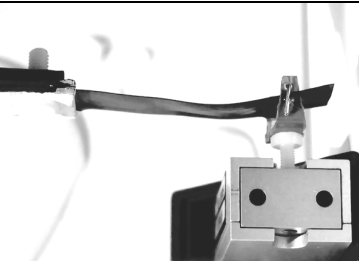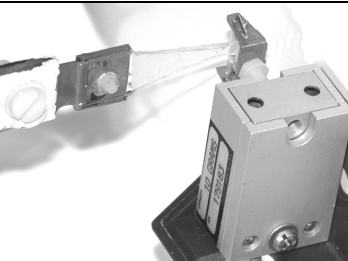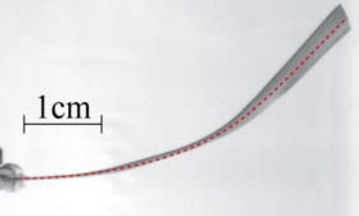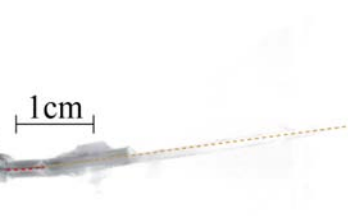
Verdu *et al* [57] proposed an advanced method based on active contour models [58]. The idea of the method is to minimize certain energy function related to the curvature of the sheet and the image data. The algorithms for tracking the motion of the sheet incorporate physical models of actual mechanical dynamic systems. However, the work only considers tracking the shape of an isolated IPMC sheet. In our case the sheet is connected to a load cell.

In our study the shape of the sheet is interpolated with a minimum variation curvature curve [59]. First geometric constraints including points and angles are specified by hand. Then the minimum variation curvature curve was found using Quasi-Newton optimization technique.

2.3.3 Two actuator configurations used in the experiments

Two different IPMC actuator configurations were used in the experiments (see Table 4). Both sheets had a notable initial curvature. The fact that IPMC actuators can be unsymmetrical is well known [36]. The table lists only properties that could be directly measured. In section 4.3 also bending stiffness and EIBM for +2V and −2V of both sheets is presented.

Table 4. Two actuator configurations used in our experiments

Parameter	Long IPMC sheet	Short IPMC sheet with an plastic elongation
Top view of the actuator		
Length of the freely bending IPMC part	50 mm	4.5 mm
Length between contacts	1.5 mm	1.5 mm
Length inside elongation	0 mm	2 mm
Width of the IPMC sheet	11 mm	11 mm
Thickness of the IPMC sheet	0.21 mm	0.21 mm
Perspective view of the actuator and the load cell		
Side view of the actuator. The initial neutral curve is denoted with the doted line		

3 THE STRUCTURE OF THE MODEL OF AN IPMC ACTUATOR

The mechanical model is only one component needed for modelling IPMC actuators. In this chapter the role of a mechanical model and a modular approach to modeling of IPMC actuators is discussed.

A physical model of an IPMC actuator can be divided into three stages. In Figure 27 one can see these stages of the model of the actuator proposed by Kanno *et al* [60]. Newbury [36] divides model parameters into three terms:

1. Electrical Terms,
2. The electromechanical Coupling Term,
3. Mechanical Terms.

Bonomo *et al* [61] propose a similar scheme to Kanno *et al* [60] where the stress generation stage and mechanical stages are merged. Chen and Tan [8] propose a scheme where electrical and stress generation stages are merged.
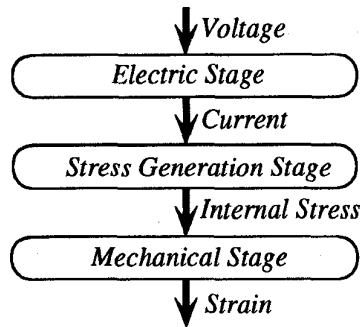
Figure 27. Three stages of the model of the actuator proposed by Kanno *et al*.

Many authors [VII,4,5,6,7,8,9,10] have proposed an electromechanical model, including electrical and stress generation stages, of an IPMC actuator. They suggest that due to the voltage applied an electrically induced bending moment or change in the free deflection curvature (in [10] it is called eigen-curvature) occurs. In this thesis it is assumed that the change of the bending moment is proportional to the change of the curvature. Hence, the electrically induced bending moment and the eigen-curvature are proportional. An example of an electromechanical model proposed in [VII] is presented in Figure 28. The mechanical model presented here can take the electrically induced bending moment as an input and give the force and shape of the sheet as an output.
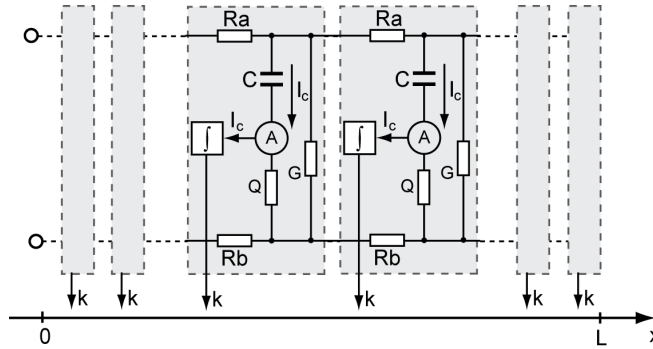
Figure 28. An electromechanical model in the form of an equivalent circuit. The charge of the capacitor is coupled with the free deflection curvature (or eigen-curvature) of the sheet.

In Figure 22, a general scheme of an IPMC actuator is presented. A more detailed scheme, showing the role of the mechanical model is presented in Figure 29. Electromechanical model converts voltage at the contacts to distribution of electrically induced bending moments along the IPMC sheet. Also current can be an input to the electromechanical model. Then mechanical model converts distribution of EIBM to the shape of the sheet (curvature) and output force. The second input to the mechanical model is the position of the actuator. That kind of a scheme corresponds to the model for predicting output force.. A scheme for predicting the position would have force as an input and position as an output.
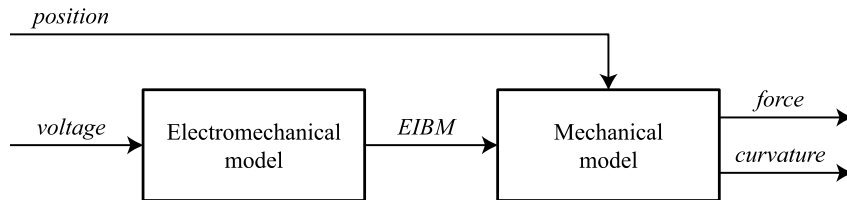
Figure 29. A detailed schema of the IPMC actuator for predicting output force.

The curvature of the sheet is not needed in precision control tasks. However, it can be used for understanding the behavior of an IPMC actuator and to draw the shape of the sheet. The mechanical model may be used to measure, how much the shape of the sheet varies. Variation of the sheet is bad for controllability of the actuator as it makes predicting the shape of the sheet in dynamic cases more difficult. Please refer to 4.3.1 for more information about shape variation.

The model presented in this thesis considers IPMC sheets with an initial curvature. As reported by [62,63], the initial curvature can change during the operation.

4 THE MECHANICAL MODEL OF AN IPMC ACTUATOR

The main contribution of this thesis is the mechanical model of an IPMC actuator. An example of the system is described in section 2.3. A diagram of the system is presented in Figure 30. An IPMC actuator in cantilever configuration (between contacts of the clamp) applies force to an object (load cell). The object can have different positions along a circular trajectory. At any given distribution of EIBM along the IPMC sheet, the model can be used to calculate position-force characteristic of the actuator. The parameters of the actuator can be identified using the model based on a position-force relationship found experimentally.
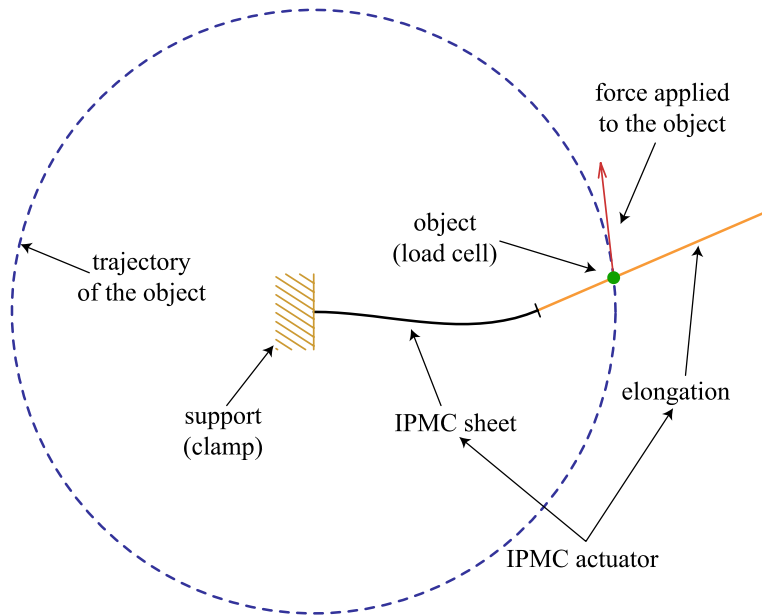
Figure 30. The diagram of the system.

This model is designed to describe elongated IPMC actuators – actuators that consist of an IPMC sheet and an absolutely rigid elongation attached to the top of it. An IPMC actuator without an elongation can be modeled as an elongated actuator with the constraint that the elongation is never in contact with the object. The elongation is infinitely long to ensure that in theory the actuator is able to reach any object regardless how far it is.

This model enables static analysis of IPMC mechanics. It enables computing the free bending curvature and force applied to an object in a static equilibrium state. It can accurately describe the quasi-static movements of an

IPMC sheet. In a dynamic case when inertial and drag forces cannot be neglected, the static model can still be used to calculate the average bending curvature and output force.

4.1   The model

An IPMC sheet between stationary contacts can be looked at as a beam in cantilever configuration. However, this theory is not the classical beam theory, because we do not assume that the beam is initially straight or deflections are small. The IPMC sheet can have a notable initial curvature and it may be bent to form a spiral.

We assume that bending is the only deformation of the beam. There is no shearing. The sheet does not change its thickness. Compressing and extending forces are considered small and are neglected. In other words:

- There is a neutral surface inside the sheet that does neither contract nor elongate. The neutral surface is assumed to be cylindrical (for example it does not consider the case in Figure 19).
- A lineal element perpendicular to the neutral surface does not elongate or contract and remains always straight.
- Along its width, the sheet can be treated at as homogeneous.

This allows us reducing the problem of 3D continuous mechanics to mechanics of a planar curve. The curve corresponds to the projection of the cylindrical neutral surface. For the IPMC sheet we assume that change of a bending moment is proportional to the change in curvature. The elongation remains always straight. The curvature of the IPMC sheet is given by

$$\forall s \leq l: \quad k(s) = k_0(s) + \frac{M_e(s) + M(s)}{B}. \tag{1}$$

This is the main equation of the model. Please refer to Table 5 for an explanation of the nomenclature and to Figure 31 for geometric definitions of parameters.

41

Table 5. Classification of the model parameters

Group name	Notation	SI Unit	Description
Task parameter	R	m	Radius of the trajectory
Actuator specific parameters	l	m	Length of the freely bending IPMC part
	$k_0(s)$	m^{-1}	Initial curvature of IPMC sheet
	B	$\text{N} \cdot \text{m}^2$	Bending stiffness of IPMC sheet
Input parameter	$M_\text{e}(s)$	$\text{N} \cdot \text{m}$	Electrically induced bending moment (EIBM)
Situation specific parameters	p	m	Position of the object on trajectory
	F	N	Force applied to the object
	$k(s)$	m^{-1}	Curvature of IPMC sheet
Supplementary notations needed to define relations between other parameters	s	m	Natural parameter of the curve
	s_F	m	Position on the sheet where force is applied
	$\hat{\alpha}$	rad	Angular deflection in the position of the object
	ϕ	rad	Angle between normal of the sheet and the tangent of the trajectory
	F_sheet	N	Force applied to the sheet
	$M(s)$	$\text{N} \cdot \text{m}$	Bending moment caused by force applied to the sheet
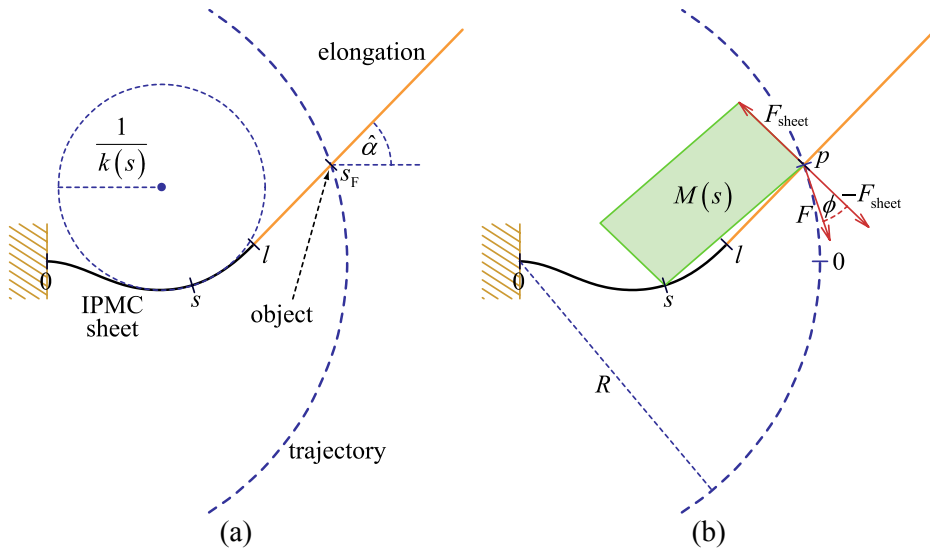
Figure 31. Geometric definitions of parameters.

The model enables describing full turns of the actuator. Different turns of the actuator can be distinguished by the value of p (and also by the angular deflection $\hat{\alpha}$). In Figure 32 one can see an actuator in two situations, a full turn apart. It illustrates that position p_i and position $p_{i+1} = p_i + 2 \cdot \pi \cdot R$ mean different turns.
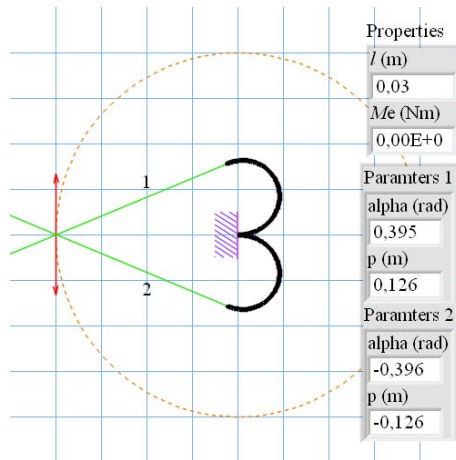
Figure 32. Same point on the trajectory – different positions on the trajectory!

For realistic results it has to hold that $l > 0$, $B > 0$, $R > 0$ and $-0.5 \cdot \pi < \phi < 0.5 \cdot \pi$. In Figure 33 there is an example of a non realistic situation, where $\phi \geq 0.5 \cdot \pi$. One can see a state of static equilibrium which could never be attained during normal operation.
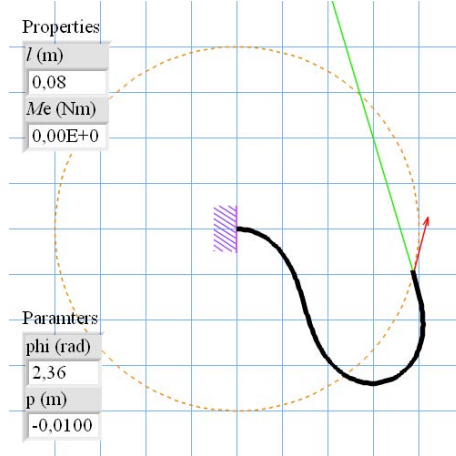
Figure 33. An example of a non realistic situation.

If one doubles the width of the IPMC sheet, it is equivalent to two sheets working in parallel. The output force would double. The same holds for stiffness and EIBM. Output force F, bending stiffness B and EIBM $M_e(s)$ are proportional to the width w of the sheet. Parameters B and $M_e(s)$, normalized to the width of the sheet characterize the properties of the IPMC material.

IPMC is a sandwich with a cracked surface and several layers with a different elastic modulus. The Young modulus of a homogeneous sheet with same dimensions and similar stiffness can be calculated using the equation

$$E = \frac{12 \cdot B}{w \cdot d^3} , \tag{2}$$

where d is thickness of the IPMC sheet. For a non-homogeneous material like IPMC this parameter is called the effective Young modulus or the equivalent Young modulus. It can be used to characterize the properties of the IPMC material. However, it is sensitive to thickness measurement errors. Therefore the use of B/w is preferred to characterize the stiffness of the material.

For more details about the model please refer to [I].

4.2 Algorithms for computing the position-force relationship

Relationship between p and F (see Table 5) is an important characteristic that helps to achieve a more efficient mechanical design of IPMC devices. This relationship is also called a position-force relationship. An analytical closed form solution for position-force relationship has not yet been found. This section describes two algorithms for solving the problem numerically. The same algorithm can also be used to find the shape of the sheet.

The mechanical model of an IPMC actuator (please see [I] for formal description) defines one-to-one relationship between the pairs (p,F) and (s_F, F_{sheet}). Both of the algorithms described in this section make use of this postulate. They search for (s_F, F_{sheet}) and use an algorithm presented in [34] to calculate the shape of the sheet. We have implemented the algorithm in LabView 8.2. Please refer to [64] for the source code. When we know the shape of the sheet, finding (p,F) is a trivial task. Both of the algorithms can be used to find position-force relationship but the inputs and outputs of the algorithms differ. Please see Table 6 for the summary of the inputs-outputs of the two algorithms.

Table 6. Inputs-Outputs of the two algorithms introduced in this section

Method	Nonlinear optimization	Mapping
Input	R, l, $k_0(s)$, B, $M_e(s)$	R, l, $k_0(s)$, B, $M_e(s)$
Data-in to specify the portion of the position-force relationship we want to find	p (or F) and initial guess of (s_F, F_{sheet})	bounds for (s_F, F_{sheet})
Output	Maximum one pair (s_F, F_{sheet})	A relationship between s_F, and F_{sheet} within given bounds
By-product	pair (p,F) and the shape of the sheet	A relationship between p and F

Both of the methods have their weaknesses because there are cases where both of them can fail. Counter examples are presented to illustrate the deficiencies of the methods. Examples are made as simple as possible. In our examples we assume a uniform EIBM along the IPMC sheet. Only l and M_e may differ for different examples. The other parameters are the same for all examples and are defined as follows: R=0.04m, $k_0(s)$=0 and B=1.21·10^{-6} N·m^2. Realistic values extracted from experiments of bending stiffness and EIBM are used.

4.2.1   Method 1: Nonlinear optimization

The most intuitive method for finding (s_F,F_{sheet}) is by using an unconstrained optimization method such as the downhill simplex method. We have implemented the algorithm in LabView 8.2. Please refer to [65] for the source code. In Figure 34 a block diagram and in Figure 35 the front panel of the algorithm for finding s and F_{sheet} using this method are presented.
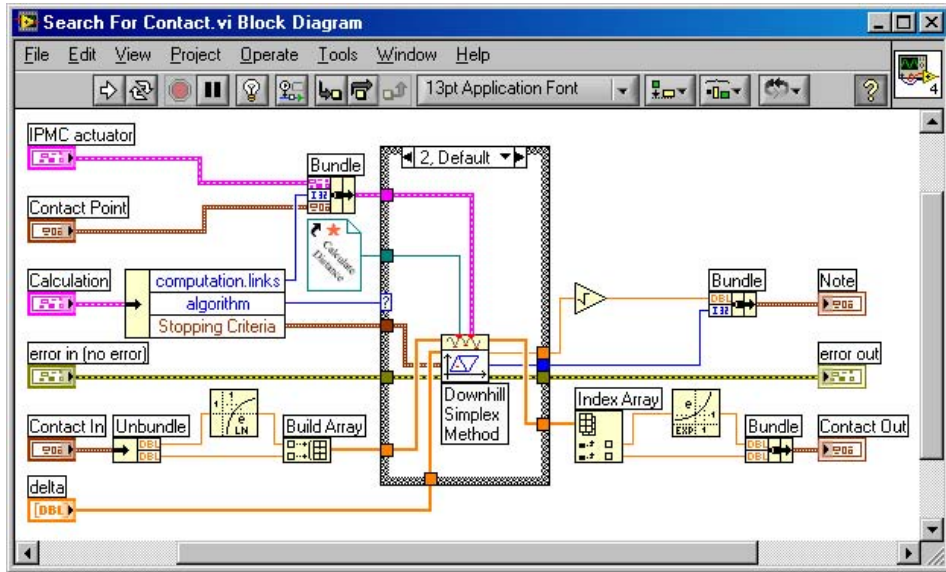

Figure 34. Block diagram of the algorithm for finding s and F_{sheet}.
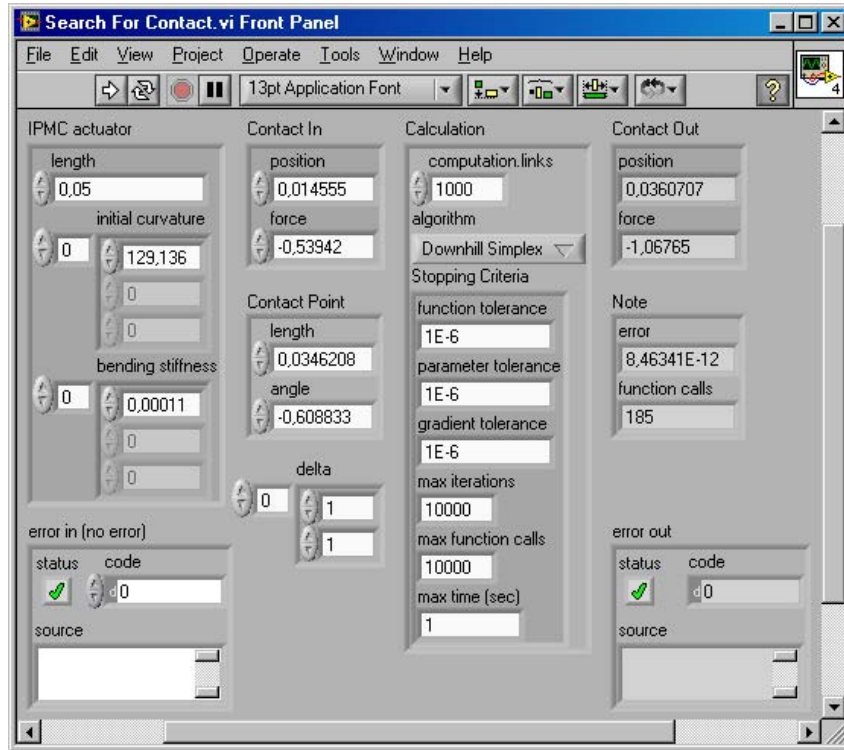
Figure 35. Front panel of the algorithm for finding s and F_{sheet}.

The task is to find (s_F, F_{sheet}) such that the point on the sheet in position s_F, would be as close to the trajectory as possible. The exact form of objective function depends on whether p or F is specified. In case p is specified, distance between the point on the trajectory in position p and point on the sheet in position s_F is minimized. In case F is specified, square distance between the trajectory and the point on the sheet in position s_F plus square difference in F is minimized.

The task can sometimes have more than one solution. This method however is able to find only one of them. Which one is found depends on the initial assumptions about of (s_F, F_{sheet}).

4.2.2   Multiple solutions

In this section counter examples for nonlinear optimization are presented. For a given position on the trajectory p there can be many forces F and pairs (s_F, F_{sheet}) which satisfy the model. This case is described in section 4.2.2.1. Also, for force applied to the object F there can be many positions p and pairs (s_F, F_{sheet})

which satisfy the model. This case is described in section 4.2.2.2. In both cases similar fluctuations in the position-force relationship appear.

4.2.2.1   1 position – 3 forces

It may happen that in the same position different forces can be applied. Such a situation is pictured in Figure 36 and the corresponding position-force relationship is given in Figure 37.

Such positions form a closed interval. There exist three different forces which satisfy the model if the position is between the endpoints of the closed interval and only two, if the position is at the endpoint of the interval.
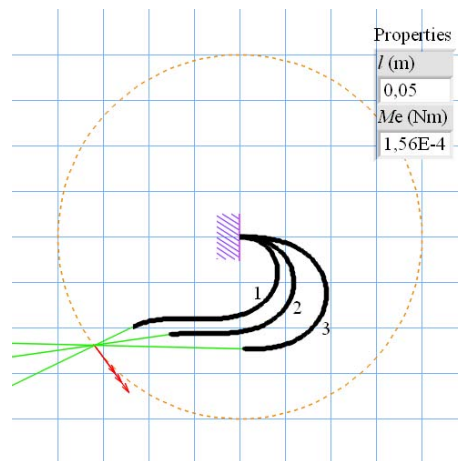
Figure 36. The shapes of the sheets, all in the same position of the trajectory.
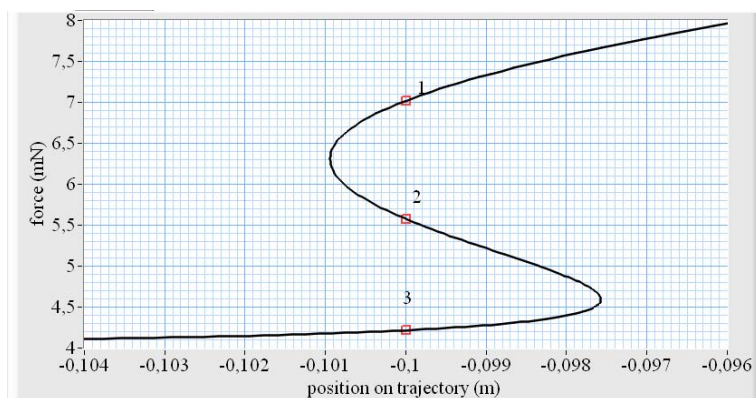
Figure 37. Position-force relationship with points corresponding to the shapes of the sheets in Figure 36.

48

4.2.2.2   1 force – 3 positions

It may happen that the same amount of force is applied to the object in different positions of the trajectory. Such a situation is pictured in Figure 38 and the corresponding position-force relationship is given in Figure 39.

Such forces form a closed interval. There exist three different positions of the trajectory if force is between the endpoints of the closed interval and only two, if force is at the endpoint of the interval.

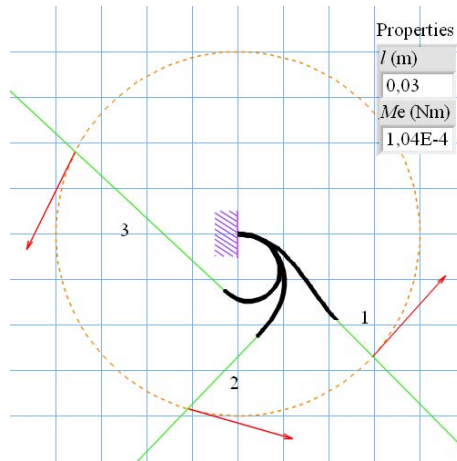**Figure 38.** The shapes of the sheets, which all apply the same amount of force.
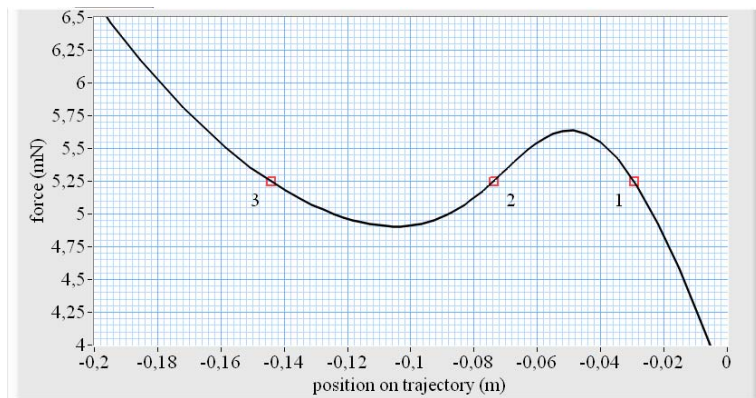

Figure 39. Position-force relationship with points corresponding to the shapes of the sheets in Figure 38.

13

4.2.3 Method 2: Mapping

The second method for calculating the position-force relationship is able to find all solutions in cases presented in the previous section. The output of the algorithm is not a single pair (s_F,F_{sheet}), but a relationship between s_F and F_{sheet} under given constraints. The relationship can be represented as a curve on s_F-F_{sheet} plane like pictured in Figure 40. The curve corresponds to pairs (s_F,F_{sheet}) for those cases where the point of the sheet in position s_F lies on the trajectory. In this section the relationship is called a curve on s_F-F_{sheet} plane and a pair (s_F,F_{sheet}) is called a point on s_F-F_{sheet} plane.

The algorithm consists of the following steps:

1. Rectangular area of s_F-F_{sheet} plane is scanned and distance between the trajectory and the point of the sheet in position s_F is recorded for each point. The distance is positive for points on one side and negative for the points on the other side of the curve on s_F-F_{sheet} plane.
2. All such pairs of points (from now on we call this a segment), with are neighbors and have distances with opposite signs, are marked. Such a segment intersects with the curve on s_F-F_{sheet} plane. In Figure 40 one can see the marked segments.
3. Using the false position method the intersection of the curve and the segment is found for each marked segment. In Figure 40 these are marked as back dots on the curve.
4. A cubic-spline interpolant is found, which crosses all the intersections. The spine is also marked in Figure 40. This curve represents the relationship between s_F and F_{sheet}.
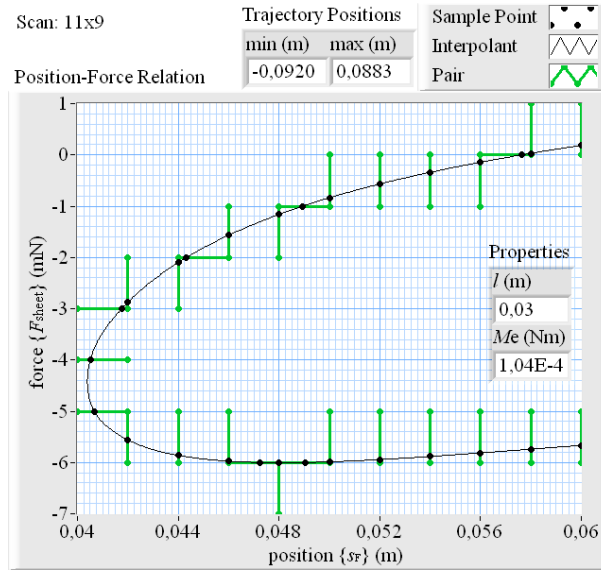
Figure 40. A scan of a rectangular area, pairs of points, intersections and cubic-spline interpolant.

We have implemented the algorithm in LabView 8.2. Please refer to [66] for the source code.

This method assumes G^1 geometric continuity (smoothness) inside the rectangular area and G^0 geometric continuity (continuity) at the border. As it is shown in the next section this assumption is not always satisfied.

4.2.4 A non G1 continuous relationship

In this section a counter example for the mapping method is presented.

In Figure 41 a relationship between s_F and F_{sheet} as a planar curve is not G^1 geometrically continuous. In Figure 42 the shapes of the sheets, corresponding to the discontinuity points are pictured. Please note that the actuator crosses the trajectory at the tip of the IPMC sheet. In Figure 43 the corresponding position-force relationship is pictured. Position-force relationship has discontinuities also.

Figure 41. A non G^1 geometrically continuous curve on s_F-F_{sheet} plane.

Figure 42. The shapes of the sheets, corresponding to the discontinuity points seen in Figure 41.
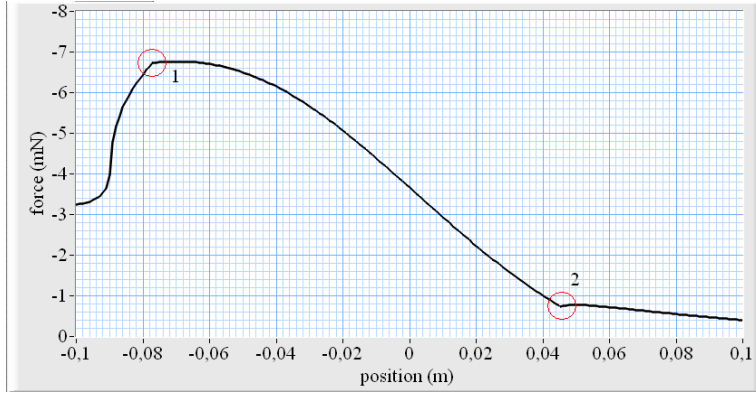
Figure 43. A discontinuous position-force relationship corresponding to the curve seen on Figure 41.

The mapping method is unable to find a non G^1 continuous relationship, but can be used to find G^1 continuous segments of such relationship.

4.3   Experimental results and discussion

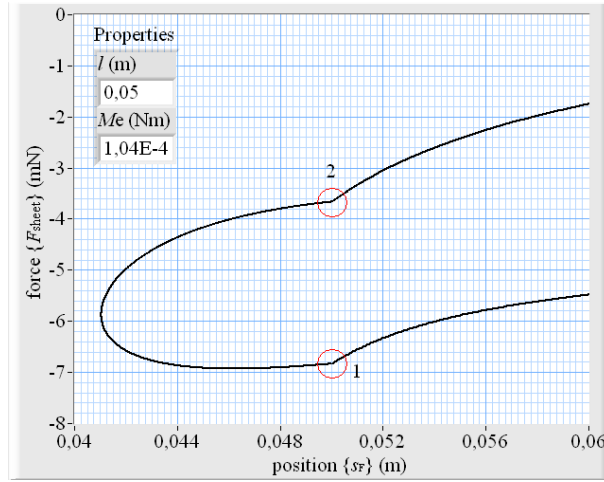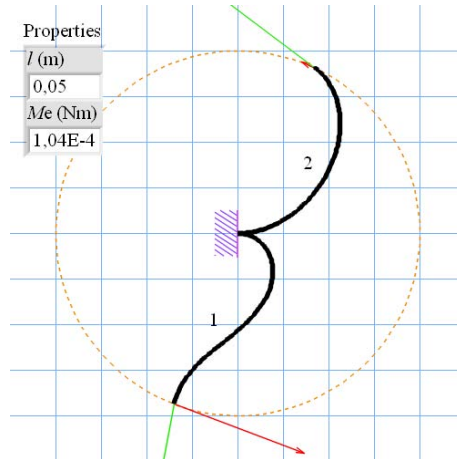To verify the proposed model and to study the behavior of two actuators described in 2.3.3, a number of experiments were conducted. The radius of the trajectory is constantly 40mm. The shape of the sheet and output force is measured in 7 different positions of the trajectory (see Figure 24) at −2V, 0V and +2V. Please refer to [I] for more details about the experiments. Please refer to [67] and [68] for the videos of the experiments of the long and the short sheet respectively in a position of the trajectory $p = 0$.

It can be concluded that the model describes accurately the behaviour of both sheets. Position-force relationship at various voltages and free deflection at various voltages is discussed in section 4.2.1. The variation of the shape of the sheet and modeling error is discussed in section 4.2.2.

Measurements of the long sheet taken in position +30 mm of the trajectory are invalid because the sheet systematically got stuck between the rolls. Please refer to Appendix B for more information.

4.3.1   The position-force relationship

In Figure 44 real and simulated output forces at different electrical stimulations can be seen. The horizontal axis corresponds to parameter p and the vertical axis to parameter F. The mean squared error of force prediction was 0.322mN for the long sheet and 0.422mN for the short sheet with an elongation.

53

14

(a)

(b)
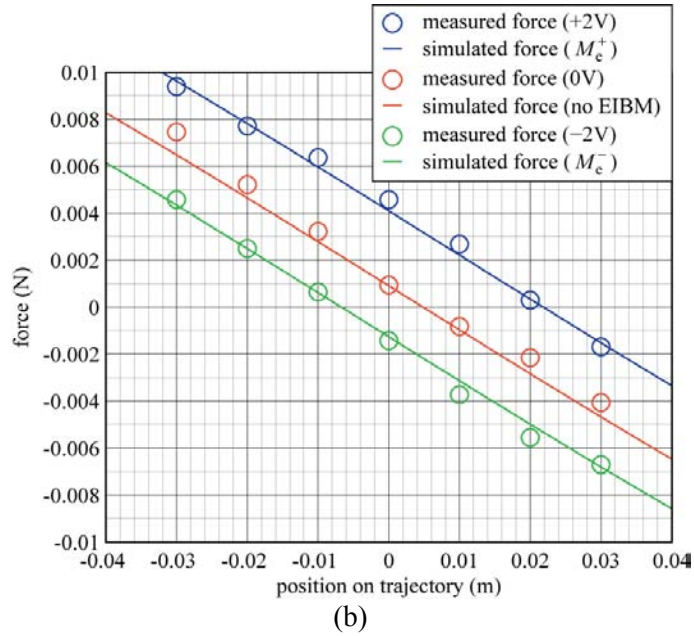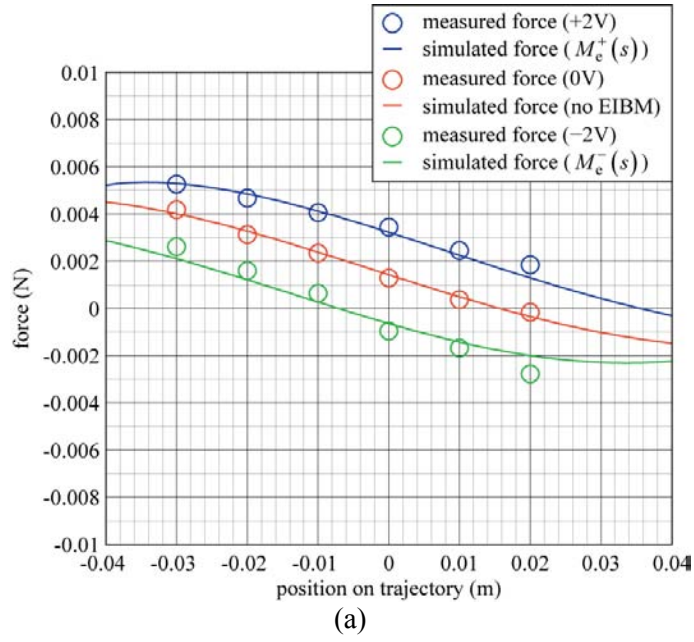
Figure 44. Real and simulated position-force relationship of the long IPMC sheet (a) and the short IPMC sheet with the plastic elongation (b).

4.3.1.1 Productivity measure

It can be noted that the mean absolute force in the initial position is approximately 1.5 times larger for the short sheet with an elongation compared to the long sheet. The maximum mean absolute free deflection (the position at zero force) on the other hand is approximately 1.5 times larger for the long sheet. As free deflection and stall tip force are equally important we propose characterizing the IPMC actuator with the product of these quantities. The result is measured in units of work (joule) and we propose calling it the productivity measure of IPMC actuator. The productivity measure is approximately equal for both actuator configurations.

4.3.1.2 Efficiency measure

As the second characteristic, an efficiency measure of the IPMC sheet is proposed. It is defined as the productivity measure divided by the area of the freely bending IPMC part. The length as well the area of the freely bending IPMC part of the long sheet is about 11 times larger than that of the short sheet. Thereby the conclusion is that the efficiency measure is approximately 11 times higher for the short sheet with elongation compared to the long sheet.

4.3.1.3 Linearity

In Figure 45 linear fits of the position-force relationship of the two actuator configurations are presented. We define linearity of the actuator as average mean square of errors of linear fits. The short sheet is about 10 times more linear than the long sheet.

(a)

(b)
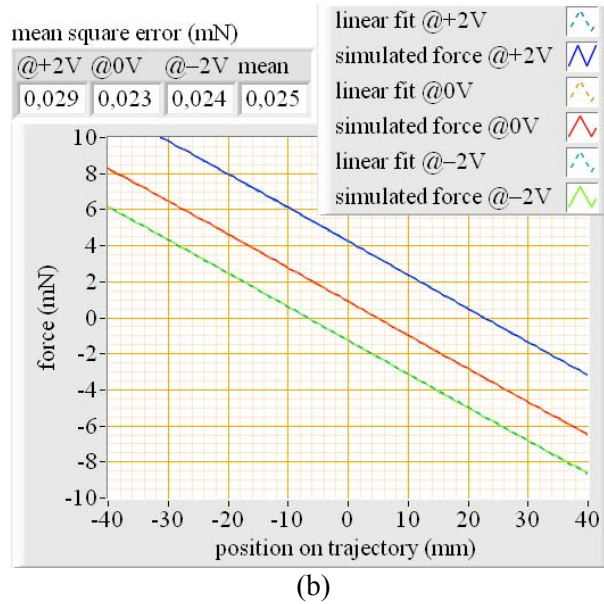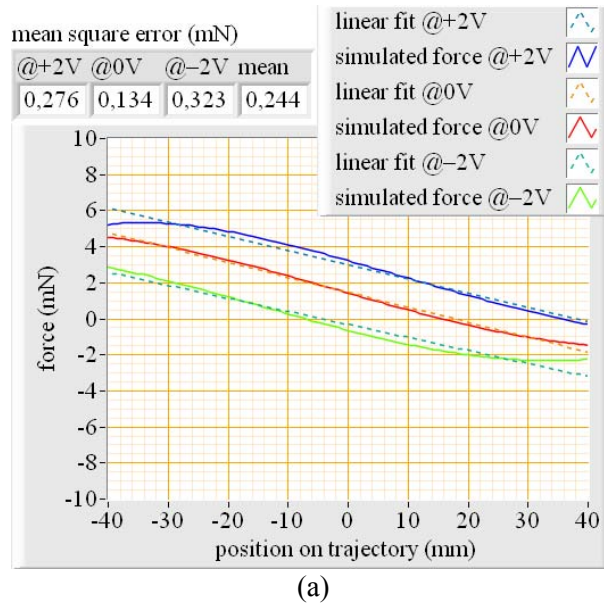
Figure 45. Simulated position-force relationship and linear fit of the relationship of the long IPMC sheet (a) and the short IPMC sheet with the plastic elongation (b).

4.3.2　Shape variation

On the videos [67,68] and in Figure 46 one can see that with different voltages the static equilibrium state of the sheet differs. In case of a long sheet the difference is large. In case of a short sheet with an elongation the difference is barely notable.
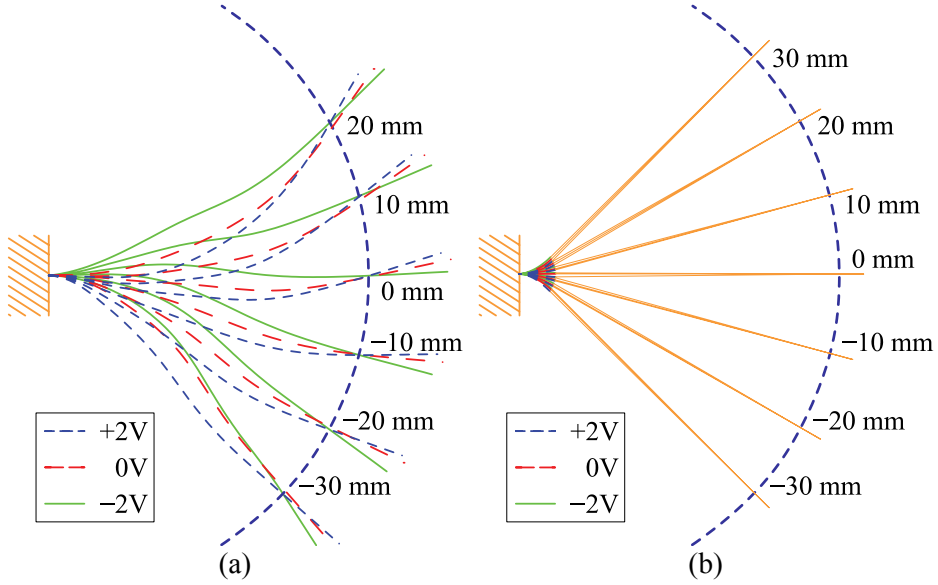
Figure 46. Neutral curves of the long sheet (a) and the short sheet (b).

Let us consider fast moving sheets and the dynamic model of the IPMC actuator. The shape of the sheet is the input parameter for calculating the output force. The less the shape of the sheet varies, the easier it is to estimate it. In case of a short sheet with an elongation the shape of the sheet does not vary so much and can be approximated as a circular arc. In case of the long sheet estimation of the shape is more difficult. We need a dynamic model of the IPMC actuator to calculate the output force based on the shape of the sheet. The static model presented here can be used to calculate the shape variation of the actuator.

We propose characterizing the shape variation of an IPMC actuator with an area between actuators at extreme opposite voltages as pictured in Figure 47. The shape of the long sheet varies on average 0.976cm^2 and the shape of the short sheet 0.086cm^2. So the shape of the long sheet varies about 11 times more than the shape of the short sheet.
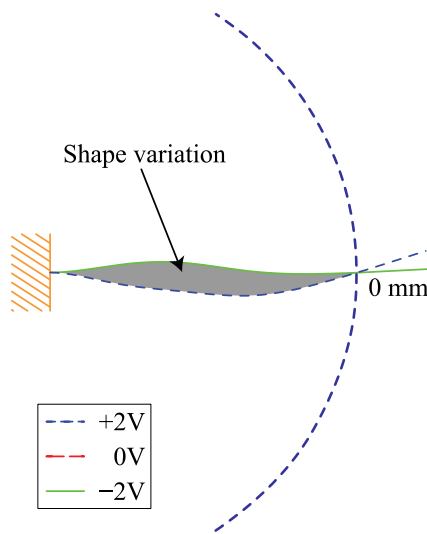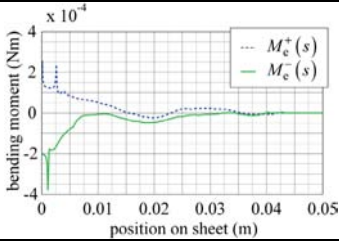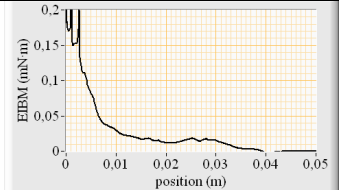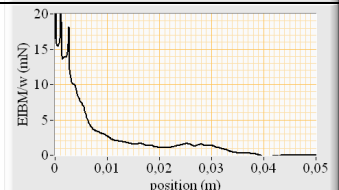
Figure 47. Shape variation of the long IPMC sheet in position zero at extreme opposite voltages.

4.4 Bending stiffness and EIBM of the two actuators

Using the model, bending stiffness and EIBM corresponding to −2V and +2V of the actuators presented in 2.3.3 could be identified. It is done based on the previously introduced experimental results. Please refer to [I] for the methodology. Table 7 summarizes the parameters extracted from the experiments.

Table 7. Parameters extracted from the experiments

Parameter	Long IPMC sheet	Short IPMC sheet with the plastic elongation
Length of the freely bending IPMC part	50.0 mm	4.50 mm
Bending stiffness	$2.03 \cdot 10^{-6} \, \text{N} \cdot \text{m}^2$	$1.21 \cdot 10^{-6} \, \text{N} \cdot \text{m}^2$
Bending stiffness normalized to the width of the sheet	$1.84 \cdot 10^{-4} \, \text{N} \cdot \text{m}$	$1.10 \cdot 10^{-4} \, \text{N} \cdot \text{m}$
Equivalent Young modulus	236 MPa	147 MPa
EIBM at +2V ($M_e^+(s)$) and −2V ($M_e^-(s)$)		$M_e^+(s) = 0.127 \, \text{mN} \cdot \text{m}$ $M_e^-(s) = -0.082 \, \text{mN} \cdot \text{m}$ EIBM for short sheet can be considered constant!
The mean absolute value of EIBM		$0.104 \, \text{mN} \cdot \text{m}$
The mean absolute value of EIBM normalized to the width of the sheet		9.470 mN

Also, in [I] simulations with a long sheet assuming constant EIBM are reported. It was concluded that this assumption is not valid. Hence these results are neglected in this review. Also, in [I] simulations with a short IPMC sheet with the plastic elongation with varying EIBM along the IPMC sheet are reported. It was concluded that permitting EIBM vary is unnecessary for describing the behaviour of the short sheet and hence is also not reflected here. Assuming constant EIBM for the short sheet is in accordance with the work of Punning et al [VII, 4]. They describe IPMC material as a lossy RC-line (see Figure 28). The longer is the actuator, the longer is the line. The longer is the line, the weaker the electrical signals get near the top of the sheet and hence EIBM decreases.

4.4.1 Comments

The following observations are made on the basis of Table 7:

1. The equivalent Young modulus proposed in this table is not much different from those proposed in [1,5,40]. The equivalent Young modulus is very sensitive to thickness measurement errors. That is one of the reasons, why our model uses bending stiffness instead.
2. The long sheet appears to be stiffer than the short sheet (although the short IPMC sheet is cut from the first part of the long IPMC sheet). It can be explained by changes in the hydration level [1,36]. Please refer to Table 4 for the side view of the short sheet. The short IPMC sheet is surrounded by water because elongation is close to the contacts and because of the surface tension of water.
3. As s increases, the varying EIBM tends to converge to zero. It can be explained by the fact that when moving toward the top of the sheet the potential between surfaces drops because of the surface resistance [VI,VII,4,43,44]. The smaller is the potential, the smaller is EIBM.
4. EIBM (both varying and constant) at voltages +2V and –2V do not have the same absolute value. This reflects the asymmetry of the material.
5. EIBM of the long IPMC sheet changes polarity or has peaks at some positions. This is caused by errors in curvature measurements.

5   A LINKED MANIPULATOR WITH IPMC JOINTS

This Chapter describes a linked manipulator using IPMC joints as pictured in Figure 48. It consists of two short IPMC sheets and two passive rigid links. The fixed end of the actuator and the first passive link have contacts through which voltage is applied to the IPMC sheets.

We argue that this design reduces the control complexity of an IPMC manipulator and increases the precision of the device. The design rationale stems from our theoretical work in material modeling presented in the previous chapter.
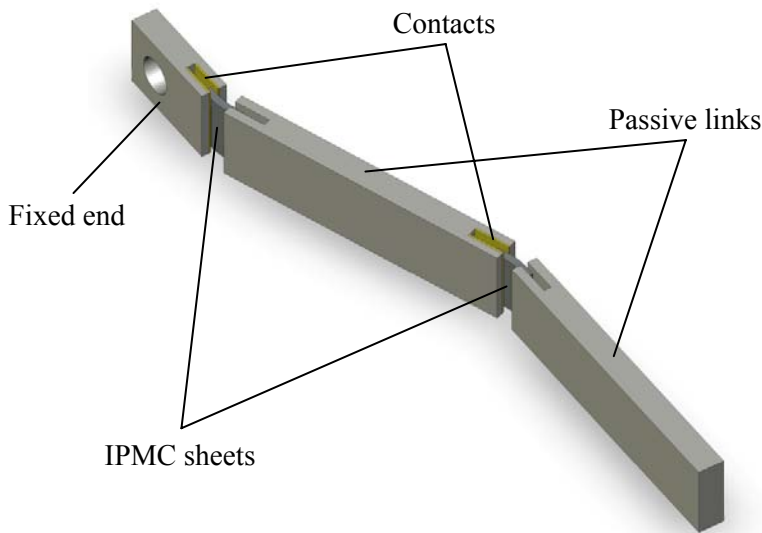
Figure 48. The design concept of the linked manipulator.

The closest related work is reported in [69] where also a multi-DOF manipulator is modeled, but the higher number of degrees of freedom is achieved with laser ablation of a single IPMC strip.

In this chapter design considerations guided by the theoretical results in material modeling are presented. We designed a manipulator prototype based on these considerations and built an experimental setup. Then experiments where conducted to test whether design considerations where justified. Only a brief description is given here. For more details please refer to [III].

16

5.1 Design considerations

The theoretical results in material modeling have guided the design considerations of the linked manipulator. The conclusions drawn from our theoretical work are discussed in this section.

5.1.1 IPMC sheet can be modeled as a hinge with joint in the middle

Short IPMC sheets are extended with rigid elongations to form a linked manipulator. In section 4.3.2 it is proposed that in such cases the shape of the sheet could be approximated with a circular arc.

As a next step, the circular arc could be replaced by a hinge. The error of the second approximation with respect to the circular arc approximation is characterized by the distance between corresponding points of the rigid link and denoted as *error*(α) (see Figure 49).
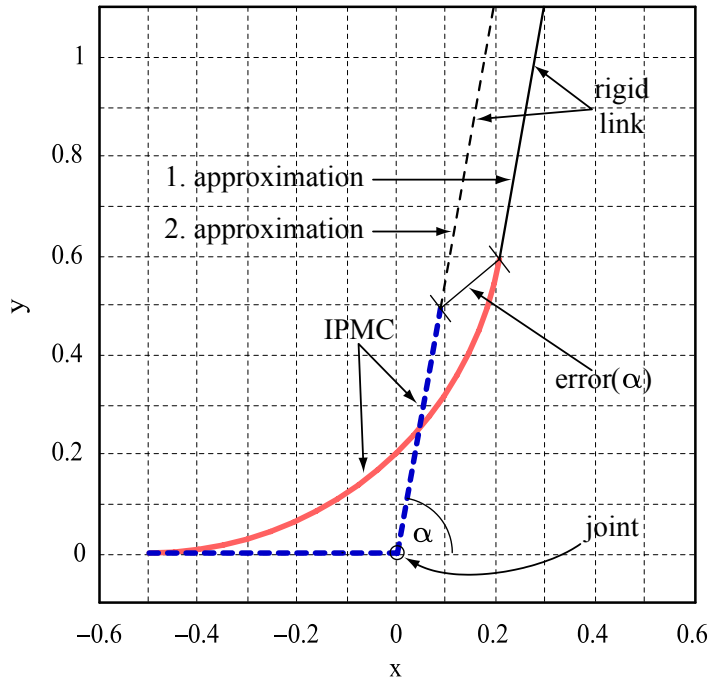
Figure 49. 1st and 2nd approximation of the link of the linked manipulator. The error of the 2nd approximation is characterized by the distance between the corresponding points of the rigid link and denoted as *error*(α). The deflection angle α=80deg and the length of the IPMC sheet *l*=1 (unitless).

The error of the second approximation *error*(α) is defined with equation (3). As one can notice, *error*(α) is proportional to the length of the IPMC sheet denoted as *l*. Dependency from α can be seen in Figure 50. We conclude that in case of small deflection angles an IPMC sheet can be modeled as a hinge with a joint.

$$error(\alpha) = l \cdot \sqrt{\cos\left(\frac{\alpha}{2}\right)^2 + \text{sinc}\left(\frac{\alpha}{2}\right)^2 - 2 \cdot \text{sinc}(\alpha)} \qquad (3)$$
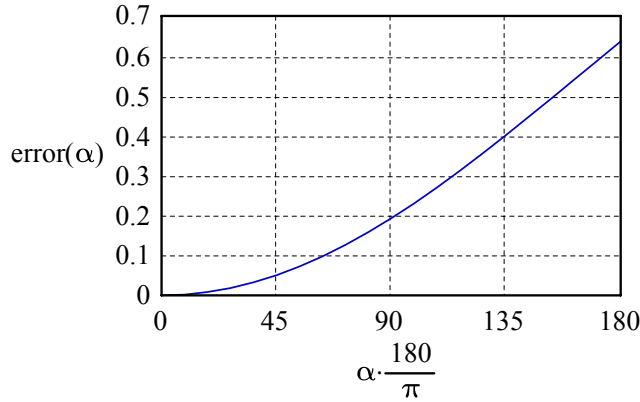
Figure 50. The error of the 2nd approximation for IPMC sheet with unit length.

5.1.2   There is a linear relationship between voltage and deflection angle

In section 4.3.1 position-force relationship of a long IPMC sheet and a short IPMC sheet with a rigid elongation is studied. It is shown that position-force relationship of a short IPMC sheet can be accurately fitted with a linear function. In case the movement of passive links is counteracted by elastic forces there is a linear relationship between the angle and output force of the IPMC sheet.

As explained in section 4.1, output force is proportional to EIBM. In section 4.4 it is shown that EIBM of a short IPMC sheet can be considered constant. From the work of Punning et al [VII], it can be derived that for the short IPMC sheets the relationship between voltage and load-free curvature of the actuator is approximately linear. Please see [III] for more details. According to the equation (1) in section 4.1 there is a linear relationship between load-free curvature and EIBM. We conclude that in case of the short IPMC sheet there is a linear relationship between voltage and deflection angle.

5.2   Experimental results and discussion

A manipulator prototype was designed based on the considerations listed above. The length of both links is 30mm. The suitable length for both IPMC joints was found to be 3mm. The length was chosen so that the linear fit of the voltage-angle relationship would be precise enough (see Figure 51).
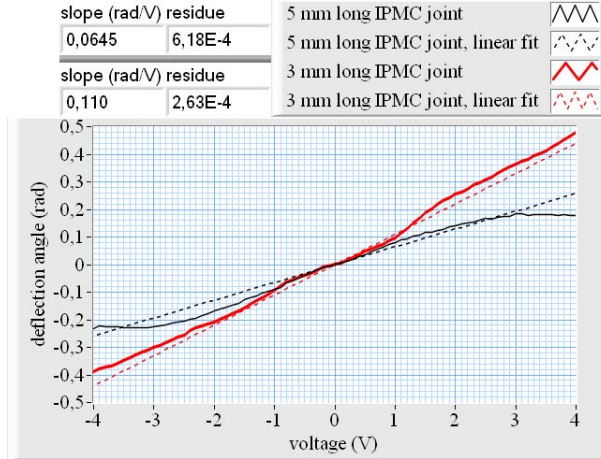
Figure 51. Calibration results of 3mm long IPMC joint where the voltage-angle relationship is nearly linear and 5mm long joint where it is non-linear.

The precision of the manipulator was measured by choosing 400 random points from the workspace of the manipulator and driving the tip of the manipulator to reach these goal points. The manipulator was modeled and controlled as consisting of a passive rigid link and an active rotating joint. Comparative experiments where conducted with 30mm long IPMC strip (such as in Figure 1). In Figure 52 the errors of the linked manipulator and the 30mm long IPMC sheet are shown. They are measured in Euclidian distance between the desired and actual end points.
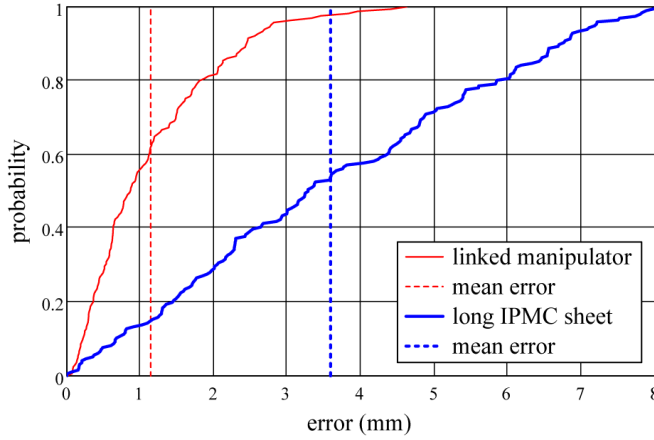
Figure 52. Cumulative error distribution of the linked manipulator and the 30mm long IPMC sheet.

The mean error of the linked manipulator is 1.14mm (standard deviation 0.92mm) and of the 30mm long IPMC sheet it is 3.59mm (standard deviation 2.20mm). Not only has the linked manipulator 2D workspace compared to the 1D workspace of the 30mm long IPMC sheet, but the linked manipulator is also 314% more accurate than the long IPMC sheet. We may thus conclude that design considerations, presented in previous section, where justified.

Also reaction times of the linked manipulator and an IPMC strip where recorded. The results show that the reaction time of the 30mm long sheet is 0.5 sec longer than of the linked manipulator. Please refer to [III] for more details.

6   CONCLUSIONS AND FUTURE WORK

6.1   Conclusions

This thesis presents a mechanical model of an IPMC (ionomeric polymer metal composite) actuator in cantilever configuration. It gives the most detailed description of the quasi-static mechanical behaviour of the actuator with a non uniform bending at large deflections reported so far. It is able to accurately describe the behavior of an IPMC actuator in cantilever configuration subjected to a concentrated load (section 4.2). Input of the modeled system is the distribution of EIBM (electrically induced bending moment). The model enables calculating output force and the shape of the sheet in every position of the trajectory.

We have presented a testbed for IPMC actuators whitch enables characterization of the actuators. It was also used to validate the model experimentally.

Newbury [36] also studies the force displacement relationship of long IPMC actuators. In case of small deformations, the force-displacement relationship was observed to be linear. In this thesis we have shown that it can also be nonlinear (see section 4.2.1).

In this thesis we have studied the impact of the use of an elongation to an IPMC actuator performance. The use of an elongation has the following advantages:

1. It avoids bending in multiple directions (Figure 19).
2. It makes the linear approximation of the position-force relationship more precise (section 4.2.1.3).
3. It makes the actuator more efficient (section 4.2.1.2).
4. The shape of the sheet varies less (section 4.2.2).
5. EIBM (and also voltage) can be considered constant along the IPMC sheet.
6. If the IPMC sheet is short enough, the voltage/maximum deflection relationship can be fitted with a linear function (see Figure 51).
7. If the IPMC part is very short with respect to the elongation, the manipulator can be described and analyzed as consisting of a passive rigid link and an active rotating joint.

The use of elongation has also a some disadvantages

1. It makes the construction of the actuator more complex,
2. It reduces the free deflection (section 4.2.1.1)

Motivated by our study on elongated sheets, a linked manipulator with IPMC joints is designed and presented in this thesis. It consists of two IPMC joints and two rigid links. It is shown that this design reduces the control

complexity of an IPMC manipulator and increases the precision and reaction speed of the device.

We have also shown that IPMC actuators enable balancing an inverted pendulum system – an inherently unstable system – for 10s. It may be concluded that the inverted pendulum is a suitable testbed for testing IMPC actuators given the physical limitations of IPMC materials.

6.2   Future Work

The mechanical model presented in this paper considers only quasi-static movements of an IPMC actuator. The next logical step would be the development of a dynamic mechanical model which would also consider inertial and drag forces.

The model could be modified to support straight trajectories like in case of an inverted pendulum system described in section 2.2, a varying bending stiffness and two or more concentrated loads.

In case of the short sheet, voltage and also EIBM can be considered constant along the IPMC sheet. This enables simplification of electromechanical models by neglecting surface resistance. The equations become simpler, as variable for the position on the sheet drops out.

As the elongation makes the linear approximation of the position-force relationship more precise, a simplified linear model for elongated sheets can be developed. The model can be coupled to the previously described simplified electromechanical model.

We have proposed a classical inverted pendulum control problem as a testbed. We suggest that if the pendulum can be balanced, then the usability of IPMC actuators for precise control tasks is proven. This could be achieved with a faster camera and the use of an elongation and a simplified linear dynamic model.

The work on the linked manipulator only addresses the open-loop control of the manipulator. However, closed loop control could improve the speed and precision of the actuator. A self-sensing actuator [14] could be used in the joints of a linked manipulator.

The design of the linked manipulator can be improved or modified. For example, more links could be added to increase the workspace even more. Also the orientation of the joints could be changed to make the manipulator work in 3D instead of 2D.

REFERENCES

[1]   Nemat-Nasser S and Thomas C 2004 **Electroactive Polymer (EAP) Actuators as Artificial Muscles—Reality, Potential and Challenges** 2nd edn, ed Y Bar-Cohen (Bellingham, WA: SPIE) chapter 6, p 171

[2]   Shahinpoor M and Kim K J 2001 **Ionic polymer–metal composites: I. Fundamentals** Smart Mater. Struct.10 819–33

[3]   K. Oguru, Y. Kawami, and H. Takenaka, "**Bending of an ion-conducting polymer film-electrode composite by an electric stimulus at low voltage**," *Trans. Journal of Micromachine Society*, vol. 5, pp. 27_30, 1992.

[4]   A. Punning, "**Electromechanical Characterization of Ion Polymer Metal Composite Sensing Actuators**," Ph.D. dissertation, Dept. of Physics, Tartu University, Estonia, 2007.

[5]   Tamagawa H, Yagasaki K and Nogata F 2002 **Mechanical characteristics of ionic polymer-metal composite in the process of self-bending** J. Appl. Phys. 92, 7614

[6]   Yagasaki K and Tamagawa H 2004 **Experimental estimate of viscoelastic properties for ionic polymer-metal composites** Physical Review E, 70, 052801

[7]   Yim W, Trabia M, Renno J, Lee J and Kim K 2006 **Dynamic Modeling of Segmented Ionic Polymer Metal Composite (IPMC) Actuator** IEEE/RSJ International Conference on Intelligent Robots and Systems, Beijing, China

[8]   Z. Chen, X. Tan, "**A Control-oriented and Physics-based Model for Ionic Polymer-Metal Composite Actuators,**" IEEE/ASME Transactions on Mechatronics, to appear, 2007

[9]   Samaranayake, B.G.L.T.; Preethichandra, D.M.G.; Alahakoon, A.M.U.K.; Kaneto, K., "**Bending Curve Modeling of Ionic Polymer Metal Composites in Soft Actuator Applications**," *Instrumentation and Measurement Technology Conference Proceedings, 2007 IEEE* , pp.1–5, 1–3 May 2007

[10]   Xiao, Y. and Bhattacharya, K., 2001, **Modeling electromechanical properties of ionic polymers**, in: Proceedings of the SPIE, Vol. 4329, pp. 292–300.

[11]   C. Bonomo, C.D. Negro, L. Fortuna, S. Graziani, "**Characterization of IPMC strip sensorial properties: preliminary results,**" in: Proc. IEEE ISCAS, 2003, pp. 816–819.

[12]   K. Sadeghipour, R. Salomon, S. Neogi, 1992 "**Development of a novel electrochemically active membrane and "smart" material based vibration sensor/damper,**" Smart Materials and Structures, Vol. 1, pp. 172–179, 1992.

[13]   Z. Chen, X. Tan, A. Will, C. Ziel, "**A Dynamic Model for Ionic Polymer-Metal Composite Sensors,**" Smart Materials and Structures, Vol. 16, pp. 1477–1488, 2007

[14]   A. Punning, M. Kruusmaa, A. Aabloo, "**A Self-sensing Ionomeric Polymer Metal Composite (IPMC) Actuator,**" Sensors and Actuators A: Physical, 136/2, 2007, pp. 656–664.

[15]   M. Shahinpoor, Y. Bar-Cohen, J. Simpson, J. Smith, **Ionic polymermetal composites (IPMCs) as biomimetic sensors, ctuators and artificial muscles – a Review**, Smart Mater. Struct. Int. J. 7 (1998) 15–30.

[16] http://www.eamex.co.jp/video/fish.wmv (07.04.2008)

[17] Ashley, S., **Artificial Muscles**, Scientific American, Vol. 289, No. 4, pp. 52–59, 2003.

[18] Bar-Cohen Y, Leary S, Yavrouian A, Oguro K, Tadokoro S, Harrison J, Smith J and Su J 1999 **Challenges to the transition of IPMC artificial muscle actuators to practical application** MRS Symposium: FF: Electroactive Polymers (Boston, MS, Nov.–Dec. 1999)

[19] Tadokoro S., Yamagami S., Ozawa M., Kimura T., Takamori T., **"Multi-DOF Device for Soft Micromanipulation Consisting of Soft Gel Actuator Elements,"** Proceedings of the 1999 IEEE International Conference on Robotics & Automation, Detroit, MI, May 1999, pp 2177–2182.

[20] Y. Bar-Cohen, S. Leary, A. Yavrouian, K. Oguro, S. Tadokoro, J. Harrison, J. Smith, and J. Su, "**Challenges to the application of IPMC as actuators of planetary mechanisms,**" presented at Smart Structures and Materials, Newport, CA, 2000.

[21] S. Guo, T. Fukuda, K. Kosuge, F. Arai, K. Oguro, M. Negoro, "**Micro catheter system with active guide wire,**" Robotics and Automation, 1995. Proceedings., 1995 IEEE International Conference on , vol.1, no., pp.79–84 vol.1, 21–27 May 1995

[22] W. Jong Yoon, Per G. Reinhall and Eric J. Seibel, **Analysis of electro-active polymer bending: A component in a low cost ultrathin scanning endoscope**, Sensors and Actuators A: Physical Volume 133, Issue 2, 12 February 2007, Pages 506–517.

[23] M. Shahinpoor and K. J Kim 2005 **Ionic polymer–metal composites: IV. Industrial and medical applications** *Smart Mater. Struct.* **14** 197–214

[24] S. J. Kim, I. T. Lee, H.-Y. Lee and Y. H. Kim 2006 **Performance improvement of an ionic polymer–metal composite actuator by parylene thin film coating** Smart Mater. Struct. 15 1540–6

[25] K. H. Low, "**Biomimetic Motion Planning of an Undulating Robotic Fish Fin**". In Journal of Vibration and Control, Vol. 12, No. 12, 1337–1359 (2006).

[26] K. Ogawa, Y. Nakabo, T. Mukai, K. Asaka, N. Ohnishi, "**A Snake-like Swimming Artificial Muscle,**" in The 2nd Conf. on Artificial Muscles, Osaka, 2004.

[27] E. Mbemmo, Z. Chen, S. Shatara, X. Tan, "**Modeling of Biomimetic Robotic Fish Propelled by An Ionic Polymer-Metal Composite Actuator,**" in Proceedings of the 2008 IEEE International Conference on Robotics and Automation, Pasadena, CA, to appear, 2008

[28] Kim B, Kim D-H, Jung J and Park J-O 2005 **A biomimetic undulatory tadpole robot using ionic polymer-metal composite actuators** Smart Mater. Struct. 14 1579–85

[29] R. Lumia and M. Shahinpoor, "**Microgripper design using electroactive polymers,**" in Smart Structures and Materials 1999: Electroactive Polymer Actuators and Devices, Y. Bar-Cohen, Ed. Bellingham, WA: SPIE, 1999, pp. 322–329.

[30] Chen Z, Shen Y, Xi N and Tan X 2007 **Integrated sensing for ionic polymer-metal composite actuators using PVDF thin films** *Smart Mater. Struct.* **16** S262–71

[31] Nakabo, Y.; Mukai, T.; Asaka, K., "**Kinematic Modeling and Visual Sensing of Multi-DOF Robot Manipulator with Patterned Artificial Muscle,**" 2005. In Proc. of the IEEE Inter. Conf. on Robotics and Automation, pp. 4315–4320, 18–22 April 2005

[32] S. Tadokoro, T. Murakami, S. Fuji, R. Kanno, M. Hattori and T. Takamori, **An elliptic friction drive element using an ICPF (ionic conducting polymer gel film) actuator**, IEEE Control Systems, 1997.

[33] S. Tadokoro, S. Yamagami, M. Ozawa, T. Kimura, and T. Takamori, "**Multi-DOF device for soft micromanipulation consisting of soft gel actuator elements,**" Proc. of IEEE Int. Conf. on Robotics and Automation, pp. 2177–2182, 1999.

[34] Bao X, Bar-Cohen Y, Chang Z and Sherrit, Stewart 2004 **Characterization of bending EAP beam actuators** Proc. SPIE Int. Soc. Opt. Eng. vol 5385 p 388–94

[35] Sangki L, Hoon C P and Kwang J K 2005 **Equivalent modeling for ionic polymer–metal composite actuators based on beam theories** Smart Mater. Struct. 14 1363–1368

[36] Newbury K 2002 **Characterization, modeling, and control of ionic polymer transducers** Dissertation Virginia Polytechnic Institute and State University

[37] Gursel Alici and Nam N. Huynh, 2006 **Predicting force output of trilayer polymer actuators**, Sensors and Actuators A: Physical Volume 132, Issue 2, 616–625.

[38] Yim W, Trabia M, Renno J, Lee J and Kim K 2006 **Dynamic Modeling of Segmented Ionic Polymer Metal Composite (IPMC) Actuator** IEEE/RSJ International Conference on Intelligent Robots and Systems, Beijing, China

[39] González C and Llorca J 2005 **Stiffness of a curved beam subjected to axial load and large displacements** International Journal of Solids and Structures 42, 1537–1545.

[40] Pugal D, Kim K J, Punning A, Kasemägi H, Kruusmaa M and Aabloo A 2007 **A Self-Oscillating Ionic Polymer-Metal Composite Bending Actuator** Journal of Applied Physics (accepted for publication).

[41] Z. Chen, X. Tan, "**A Control-oriented and Physics-based Model for Ionic Polymer-Metal Composite Actuators,**" IEEE/ASME Transactions on Mechatronics, to appear, 2007

[42] Samaranayake, B.G.L.T.; Preethichandra, D.M.G.; Alahakoon, A.M.U.K.; Kaneto, K., "**Bending Curve Modeling of Ionic Polymer Metal Composites in Soft Actuator Applications,**" *Instrumentation and Measurement Technology Conference Proceedings, 2007 IEEE* , pp.1–5, 1–3 May 2007

[43] M. Shahinpoor, K.J. Kim, "**The Effect of Surface-Electrode Resistance on the Performance of Ionic Polymer-Metal Composite (IPMC) Artificial Muscles**" Smart Materials and Structures Journal – vol. 9, no. 4, pp. 543–551 (2000)

[44] Punning A, Kruusmaa M and Aabloo A 2007 **Surface resistance experiments with IPMC sensors and actuators** Sensors Actuators A 133 200–9

[45] Campolo, D.; Sahai, R.; Fearing, R.S. (2003) **Development of piezoelectric bending actuators with embedded piezoelectric sensors for micromechanical flapping mechanisms**, ICRA '03, ,14–19 Sept. 2003. Page(s):3339 – 3346 vol.3

[46] J. M. Gere and S. Timoshenko, **Mechanics of Materials**, 4th ed. Boston, MA: PWS Publishing Company, 1997.

[47] http://www.ims.ut.ee/~mart/Thesis/Ray.vi (May 6, 2008)

[48] http://www.ut.ee/~maarjakr/ray (June 1,2004)

[49] http://www.ims.ut.ee/~mart/Thesis/IPController.zip (May 6, 2008)

[50] C. Kothera, **Characterization, Modeling, and Control of the Nonlinear Actuation Response of Ionic Polymer Transducers**. PhD thesis, Virginia Polytechnic Institute and State University, September 2005.

[51] K. Mallavarapu, **Feedback control of ionic polymer actuators**, Master's Thesis, Virginia Polytechnic Institute and State University, July 2001.

[52] N. D. Bhat, **Modeling and Precision Control of Ionic Polymer Metal Composite**, Master's Thesis, Pune University, August 2003.

[53] Kwansoo Yun and Won-jong Kim 2006 **Microscale position control of an electroactive polymer using an anti-windup scheme** Smart Mater. Struct. 15 924–930

[54] Sunhyuk Kang, Jongho Shin, Seong Jun Kim, H Jin Kim and Yong Hyup Kim 2007 **Robust control of ionic polymer–metal composites** Smart Mater. Struct. 16 2457–2463

[55] http://math.ut.ee/~marte/ip/experiment01.mpg (July 1, 2006)

[56] Bar-Cohen, Y., X. Bao, S. Sherrit, S. Lih, "**Characterization of the electro-mechanical properties of Ionomeric Polymer-Metal Composite (IPMC),**" Proc. of SPIE, v 4695, p 286–293, 2002.

[57] R. Verdu, J. Morales, A.J. Fernandez-Romero, M.T. Cortes, T.F. Otero, L. Weruaga "**Mechanical Characterization of Artificial Muscles with Computer Vision**" Smart Structures and Materials 2002: Electroactive Polymer Actuators and Devices (EAPAD), edited by Y. Bar-Cohen, Proceedings of SPIE Vol. 4695 lk. 253–261

[58] M. Kass, A. Witkin, and D. Terzopoulos, "**Snakes: Active contour models**," International Journal of Computer Vision 1(4), p. 321:331, 1998.

[59] Moreton H P 1992 **Minimum Curvature Variation Curves, Networks, and Surfaces for Fair Free-Form Shape Design** PhD thesis U. of California Berkeley

[60] Kanno R, Tadokoro S, Takamori T, Hattori M and Oguro K 1996 **Linear approximate dynamic model of an ICPF actuator** Proc. IEEE Int. Conf. on Robotics and Automation (Minneapolis) vol 1, pp 219–25

[61] C Bonomo, L Fortuna, P Giannone, S Graziani and S Strazzeri 2007 **A nonlinear model for ionic polymer metal composites as actuators** *Smart Mater. Struct.* **16** 1–12

[62] Z. Chen, X. Tan, M. Shahinpoor, "Quasi-static Positioning of Ionic Polymer-Metal Composite (IPMC) Actuators," Proceedings of the IEEE/ASME International Conference on Advanced Intelligent Mechatronics, Monterey, CA, pp. 60–65, 2005

[63] **Electrically induced permanent strain in ionic polymer-metal composite actuators** Kenneth M. Newbury and Donald J. Leo Proc. SPIE Int. Soc. Opt. Eng. 4695, 67 (2002)

[64] http://www.ims.ut.ee/~mart/Thesis/IPMCMechanics.zip
      ->Get Curvature.vi (May 6, 2008)

[65] http://www.ims.ut.ee/~mart/Thesis/IPMCMechanics.zip
      ->Search For Contact.vi (May 6, 2008)

[66] http://www.ims.ut.ee/~mart/Thesis/IPMCMechanics.zip
      ->Get Segment of Relation.vi (May 6, 2008)

[67] http://www.ims.ut.ee/www-public/IPMCMechanics/IPMC_Mechanics_Long.avi
      (November 22, 2007)

[68] http://www.ims.ut.ee/www-public/IPMCMechanics/IPMC_Mechanics_Short.avi
      (November 22, 2007)

[69] Y. Nakabo, T. Mukai, K. Asaka, "**Kinematic modeling and visual sensing of multi-DOF robot manipulator with patterned artificial muscle**", Proc. IEEE Int. Conf. Robotics and Automation (ICRA 2005), Barcelona, pp.4326–4331.

SUMMARY IN ESTONIAN

IPMC TÄITURITE MEHAANIKA MODELLEERIMINE SUURTE PAINETE KORRAL

Doktoritöö on rakendusliku suunitlusega. Uuritud on elektrivoolu toimel painduvate materjalide modelleerimist ja juhtimist. Kasutati materjali, mida inglise keeles nimetatakse Ionomeric Polymer-Metal Composite (edaspidi IPMC). Välimuselt meenutab IPMC mõlemalt poolt õhukese metallikihiga kaetud kilet. Metallikihtide vahel elektripinge rakendamisel (näiteks 2V) kile paindub. IPMC ehitust ja tööpõhimõtet on täpsemalt kirjeldatud väitekirja 1. osa alguses.

IPMC materjalist valmistatud täituritel on mitmeid häid omadusi, nagu madal tööpinge ja suur paine. IPMC täiturid rikastaks oluliselt masinaehituseks kasutatavate täiturite valikut, luues uusi konstruktsioonivõimalusi ja muutes paljud seadmed konstruktsiooni poolest lihtsamaks. Potentsiaalne kasutus-valdkond ulatub mänguasjadest kosmosetehnikani. Alaosas 1.1. on toodud põhjalik ülevaade IPMC materjali omadustest ja kasutusvaldkonnast.

Väitekirja 2. osas uuritakse IPMC täituri erinevaid konfiguratsioone ja tehakse järeldusi täituri oleku ja rakendatava jõu mõõdetavuse kohta nendes konfiguratsioonides. Alaosas 2.1. on vaatluse all robotkala. Katsetest selgus, et IPMC täiturid suudavad sellist kala edasi viia, aga täiturite täpne liikumine polnud kahjuks mõõdetav. Järgmisena vaadeldud inverteeritud pendli süsteemis on täituri positsioon juba mõõdetav, aga mõõdetav pole täituri poolt rakendatud jõud. Katseid inverteeritud pendliga kirjeldatakse täpsemalt väitekirja alaosas 2.2. Eelpool mainitud puudused õnnestus likvideerida kolmandal katsel. Alaosas 2.3. kirjeldatakse süsteemi, kus IPMC täituri asend on ette antav ja rakendatud jõud kergesti mõõdetav. Seda süsteemi kasutatakse IPMC omaduste kindakstegemisel ja väitekirjas kirjeldatud IPMC täituri mudeli valideerimisel.

Seniajani on valdav enamus IPMC rakendusi laboratoorsete katsetuste tasemel. IPMC täiturid avastati alles 1992. aastal ja pole veel jõutud selgeks teha, kuidas seda materjali täpselt modelleerima ja juhtima peaks. IPMC täituri mudelit võib käsitleda kaheosalisena: a) elektromehaaniline osa ja b) mehaani-line osa. Elektromehaaniline mudel kirjeldab, kuidas rakendatud elektripinge toimel tekib materjalis paindemoment. Sealjuures võivad voolu poolt tekitatud paindemomendid riba erinevates punktides erineda. Mehaaniline mudel kirjel-dab riba käitumist etteantud voolu poolt põhjustatud paindemomentide jaotuse korral pikki riba. IPMC täituri mudeli struktuuri kirjeldus on esitatud 3. osas. Väitekirjas keskendustakse peaasjalikult IPMC täituri mehaanika uurimisele.

IPMC täituri mehaanika matemaatiline kirjeldamine on üldiselt kolme-mõõtmelise pideva mehaanika ülesanne. Teatud eeldustel võib aga ülesande

73

taandada IPMC riba kuju esitava tasandilise kõvera liikumise uurimisele. Väitekirja 4. osas tutvustataksegi just sellist mudelit. Tegemist on seniloodutest kõige täielikuma IPMC täituri mehaanilise mudeliga. See kirjeldab IPMC täituri kuju ja rakendatavat jõudu suurtel painetel ja voolu poolt põhjustatud ebaühtlaselt jaotunud paindemomendi korral. IPMC täitur koosneb lihtsamal juhul IPMC ribast, aga IPMC täitur võib koosneda ka IPMC tükist ja selle külge kinnitatud jäigast pikendusest. Tutvustatud mudeliga on võimalik kirjeldada mõlemat juhtu. Mudeli korrektsuse testimiseks sooritati alaosas 2.3. kirjeldatud süsteemiga seeria eksperimente ning võrreldi eksperimentide tulemusi simulatsioonidega. Saadud tulemusest tehti järeldus, et mudel on korrektne.

Pikenduse kasutamise idee edasiarendusena esitatakse 5. osas lülimanipulaatori konstruktsioon. See koosneb kahest jäigast lülist ja kahest IPMC materjalist liigendist. Sisuliselt on kaks pikendusega IPMC täiturit kokku ühendatud. Nii saavutatakse suurem tööpiirkond kui ühe täituriga. Katseliselt tõestatakse, et lülimanipulaator võib olla täpsem ja kiirem kui traditsiooniline IPMC riba kujul täitur.

Kuigi pikenduse idee on lihtne ja varem tuntud, pole seinajani selle kasutamist IPMC täiturite ehitamisel põhjalikumalt uuritud. Väitekirjas on toodud mitmeid argumenteeritud väiteid pikenduse heade ja halbade omaduste kohta. Katsete ja simulatsioonide põhjal võib näiteks järeldada, et pikenduse kasutamine muudab positsiooni-jõu suhtele lineaarse lähenduse täpsemaks. Täielik ülevaade pikenduse kasutamise headest ja halbadest omadustest on toodud väitekirja kokkuvõtvas alaosas 6.1.

Väitekirjas esitatud mehaaniline mudel on staatiline ja sobib seega ainult IPMC täituri aeglase liikumise kirjeldamiseks. Kiiremate liigutuste tarvis oleks vaja koostada dünaamiline mudel. Sellest täpsemalt ja lisaks muudest edasistest uurimistöö võimalustest on kirjutatud alaosas 6.2.

ACKNOWLEDGEMENTS

I wish to thank my supervisors Maarja Kruusmaa, Alvo Aabloo and Jan Willemson for their suggestions and all-around support.

I am also very grateful to my colleagues Andres Punning and Urmas Johanson for their interest in my work. Their vast scientific knowledge has been of a grate help.

Also, I would like to thank my parents Sirje, Tõnu and my sister Ülle, whose never-ending encouragement and support has helped me to accomplish this thesis.

APPENDIX A.

To compare classical linear beam theory and mechanical model of IPMC beam presented in [I], beam deformations under different concentrated normal loads were calculated. For results, please refer to Figure 5. To calculate the shape of the beam with the model in [I], an algorithm described in section 4.2. was used. The shape of the beam, using classical linear beam theory, was calculated as follows.

Let B be denote bending stiffness, l length of a beam and F concentrated normal load at the end of the beam. When the tip of the beam is loaded, the beam bends and points of neutral curve of the beam relocate. In classical linear beam theory, axial displacement of points is neglected. We denote normal displacement of points as $y(x)$. The tangential angle of the beam is approximated as $y'(x)$ and the curvature as $y''(x)$. According to the main equation of linear beam theory

$$y''(x) = \frac{F \cdot (l - x)}{B}.$$ (4)

By integrating and considering that tangential angle at the contacts is zero $y'(0) = 0$, we get

$$y'(x) = \frac{F}{B} \cdot \left(l \cdot x - \frac{1}{2} \cdot x^2 \right).$$ (5)

By integrating and considering that the beam starts from point zero $y(0) = 0$, we get

$$y(x) = \frac{F}{B} \cdot \left(\frac{1}{2} \cdot l \cdot x^2 - \frac{1}{6} \cdot x^3 \right).$$ (6)

This simple equation gives us the shape of the beam according to the classical linear beam theory. Nonlinear beam theory, like the one introduced in [I], does not give us such simple analytical equation. On the other hand, nonlinear beam theory is more precise in case of large deformations (see Figure 5).

APPENDIX B.

In this section a problem with a long IPMC sheet is discussed. In the outermost position +30 mm of the trajectory (Figure 53) the sheet systematically got stuck.

To ensure frictionless contact between the IPMC actuator and the load cell, the actuator is held between the rolls (see Figure 23). The gap between the rolls is bigger than thickness of the material, to enable ϕ values different than zero. Please refer to Table 5 and Figure 31 (b) for the definitions of ϕ. The mechanical construction has to consider different values of ϕ. However, the gap can not be too large or the connection would allow for backlash. So starting at a certain ϕ value the sheet will not be able to move freely between the rolls.

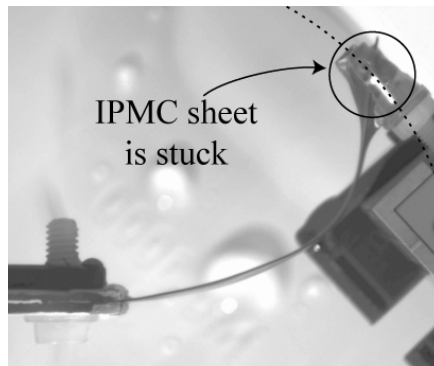**Figure 53.** The sheet does not fit to move freely between the rolls of the load cell.

PUBLICATIONS

I

A mechanical model of a non-uniform Ionomeric Polymer Metal Composite (IPMC) actuator

M. Anton, A. Aabloo, A. Punning, M. Kruusmaa, Smart materials and structures, 17(2), 2008.

II

Validating Usability of Ionomeric Polymer-Metal Composite Actuators for Real Life Applications

III

A Linked Manipulator with Ion-Polymer Metal Composite (IPMC) Joints for Soft- and Micromanipulation

IV

Towards a biomimetic EAP robot

CURRICULUM VITAE

Mart Anton

Date and place of birth:	March 6. 1979, Tartu, Estonia
Citizenship:	Estonian
Address:	Tartu Ülikooli Tehnoloogiainstituut
	Nooruse 1,50411 Tartu, Estonia
Phone:	+372 7374831, +372 5234098
e-mail:	mart.anton@ut.ee

Education

1994–1997	Hugo Treffneri Gümnaasium
1997–2001	Tartu Ülikool, Bachelor in Computer Science
2001–2003	Tartu Ülikool, MSc in Computer Science

Employment

2001–2004	Urania Com OÜ, computer programmer

Scientific work

The main fields of interest are modeling, control and application of electroactive polymers (EAP) and bending EAP-s.

Honours/Awards

- Estonian Information Technology Foundation, The stipend for doctoral student of information and communication technology of Tiger University, 2005.
- Estonian Information Technology Foundation, The stipend for doctoral student of information and communication technology of Tiger University, 2007.
- Tartu University Foundation, Ernst Jaakson Memorial Foundation Stipend, 2008.

CURRICULUM VITAE IN ESTONIAN

Mart Anton

Sünni aeg ja –koht: 06.03.1979, Tartu, Eesti
Kodakonsus: Eesti
Aadress: Tartu Ülikooli Tehnoloogiainstituut
                        Nooruse 1, 50411 Tartu, Eesti
Telefon: +372 7374831, +372 5234098
e-post: mart.anton@ut.ee

Haridus

1994–1997   Hugo Treffneri Gümnaasium
1997–2001   Tartu Ülikool, informaatika bakalaureus
2001–2003   Tartu Ülikool, informaatika magister

Teenistuskäik

2001–2004   Urania Com OÜ, programmeerija

Teadustegevus

Peamisteks uurimisvaldkondadeks on elektroaktiivsete polümeeride – täpsemalt elektrivoolu toimel painduvate materjalide – modelleerimine, juhtimine ja rakendamine.

Tunnustused

- Eesti Infotehnoloogia Sihtasutus, Tiigriülikooli stipendium info- ja kommunikatsioonitehnoloogia (IKT) doktorantidele, 2005.
- Eesti Infotehnoloogia Sihtasutus, Tiigriülikooli stipendium info- ja kommunikatsioonitehnoloogia (IKT) doktorantidele, 2007.
- Tartu Ülikooli Sihtasutus, Ernst Jaaksoni mälestusfondi stipendium, 2008.

DISSERTATIONES MATHEMATICAE
UNIVERSITATIS TARTUENSIS

1. **Mati Heinloo.** The design of nonhomogeneous spherical vessels, cylindrical tubes and circular discs. Tartu, 1991, 23 p.
2. **Boris Komrakov.** Primitive actions and the Sophus Lie problem. Tartu, 1991, 14 p.
3. **Jaak Heinloo.** Phenomenological (continuum) theory of turbulence. Tartu, 1992, 47 p.
4. **Ants Tauts.** Infinite formulae in intuitionistic logic of higher order. Tartu, 1992, 15 p.
5. **Tarmo Soomere.** Kinetic theory of Rossby waves. Tartu, 1992, 32 p.
6. **Jüri Majak.** Optimization of plastic axisymmetric plates and shells in the case of Von Mises yield condition. Tartu, 1992, 32 p.
7. **Ants Aasma.** Matrix transformations of summability and absolute summability fields of matrix methods. Tartu, 1993, 32 p.
8. **Helle Hein.** Optimization of plastic axisymmetric plates and shells with piece-wise constant thickness. Tartu, 1993, 28 p.
9. **Toomas Kiho.** Study of optimality of iterated Lavrentiev method and its generalizations. Tartu, 1994, 23 p.
10. **Arne Kokk.** Joint spectral theory and extension of non-trivial multiplicative linear functionals. Tartu, 1995, 165 p.
11. **Toomas Lepikult.** Automated calculation of dynamically loaded rigidplastic structures. Tartu, 1995, 93 p. (in Russian).
12. **Sander Hannus.** Parametrical optimization of the plastic cylindrical shells by taking into account geometrical and physical nonlinearities. Tartu, 1995, 74 p.
13. **Sergei Tupailo.** Hilbert's epsilon-symbol in predicative subsystems of analysis. Tartu, 1996, 134 p.
14. **Enno Saks.** Analysis and optimization of elastic-plastic shafts in torsion. Tartu, 1996, 96 p.
15. **Valdis Laan.** Pullbacks and flatness properties of acts. Tartu, 1999, 90 p.
16. **Märt Põldvere.** Subspaces of Banach spaces having Phelps' uniqueness property. Tartu, 1999, 74 p.
17. **Jelena Ausekle.** Compactness of operators in Lorentz and Orlicz sequence spaces. Tartu, 1999, 72 p.
18. **Krista Fischer.** Structural mean models for analyzing the effect of compliance in clinical trials. Tartu, 1999, 124 p.

19. **Helger Lipmaa.** Secure and efficient time-stamping systems. Tartu, 1999, 56 p.
20. **Jüri Lember.** Consistency of empirical k-centres. Tartu, 1999, 148 p.
21. **Ella Puman.** Optimization of plastic conical shells. Tartu, 2000, 102 p.
22. **Kaili Müürisep.** Eesti keele arvutigrammatika: süntaks. Tartu, 2000, 107 lk.
23. **Varmo Vene.** Categorical programming with inductive and coinductive types. Tartu, 2000, 116 p.
24. **Olga Sokratova.** Ω-rings, their flat and projective acts with some applications. Tartu, 2000, 120 p.
25. **Maria Zeltser.** Investigation of double sequence spaces by soft and hard analitical methods. Tartu, 2001, 154 p.
26. **Ernst Tungel.** Optimization of plastic spherical shells. Tartu, 2001, 90 p.
27. **Tiina Puolakainen.** Eesti keele arvutigrammatika: morfoloogiline ühestamine. Tartu, 2001, 138 p.
28. **Rainis Haller.** *M(r,s)*-inequalities. Tartu, 2002, 78 p.
29. **Jan Villemson.** Size-efficient interval time stamps. Tartu, 2002, 82 p.
30. **Eno Tõnisson.** Solving of expession manipulation exercises in computer algebra systems. Tartu, 2002, 92 p.
31. **Mart Abel.** Structure of Gelfand-Mazur algebras. Tartu, 2003. 94 p.
32. **Vladimir Kuchmei.** Affine completeness of some ockham algebras. Tartu, 2003. 100 p.
33. **Olga Dunajeva.** Asymptotic matrix methods in statistical inference problems. Tartu 2003. 78 p.
34. **Mare Tarang.** Stability of the spline collocation method for volterra integro-differential equations. Tartu 2004. 90 p.
35. **Tatjana Nahtman.** Permutation invariance and reparameterizations in linear models. Tartu 2004. 91 p.
36. **Märt Möls.** Linear mixed models with equivalent predictors. Tartu 2004. 70 p.
37. **Kristiina Hakk.** Approximation methods for weakly singular integral equations with discontinuous coefficients. Tartu 2004, 137 p.
38. **Meelis Käärik.** Fitting sets to probability distributions. Tartu 2005, 90 p.
39. **Inga Parts.** Piecewise polynomial collocation methods for solving weakly singular integro-differential equations. Tartu 2005, 140 p.
40. **Natalia Saealle.** Convergence and summability with speed of functional series. Tartu 2005, 91 p.
41. **Tanel Kaart.** The reliability of linear mixed models in genetic studies. Tartu 2006, 124 p.

42. **Kadre Torn.** Shear and bending response of inelastic structures to dynamic load. Tartu 2006, 142 p.
43. **Kristel Mikkor.** Uniform factorisation for compact subsets of Banach spaces of operators. Tartu 2006, 72 p.
44. **Darja Saveljeva.** Quadratic and cubic spline collocation for Volterra integral equations. Tartu 2006, 117 p.
45. **Kristo Heero.** Path planning and learning strategies for mobile robots in dynamic partially unknown environments. Tartu 2006, 123 p.
46. **Annely Mürk.** Optimization of inelastic plates with cracks. Tartu 2006. 137 p.
47. **Annemai Raidjõe.** Sequence spaces defined by modulus functions and superposition operators. Tartu 2006, 97 p.
48. **Olga Panova.** Real Gelfand-Mazur algebras. Tartu 2006, 82 p.
49. **Härmel Nestra.** Iteratively defined transfinite trace semantics and program slicing with respect to them. Tartu 2006, 116 p.
50. **Margus Pihlak.** Approximation of multivariate distribution functions. Tartu 2007, 82 p.
51. **Ene Käärik.** Handling dropouts in repeated measurements using copulas. Tartu 2007, 99 p.
52. **Artur Sepp.** Affine models in mathematical finance: an analytical approach. Tartu 2007, 147 p.
53. **Marina Issakova.** Solving of linear equations, linear inequalities and systems of linear equations in interactive learning environment. Tartu 2007, 170 p.
54. **Kaja Sõstra.** Restriction estimator for domains. Tartu 2007, 104 p.
55. **Kaarel Kaljurand.** Attempto controlled English as a Semantic Web language. Tartu 2007, 162 p